Air Duct Systems For Roadway Stabilization Over Permafrost Areas

FINAL REPORT

By

John P. Zarling, P.E.
Professor of Mechanical Engineering
University of Alaska Fairbanks

Billy Connor, P.E.
Senior Research Engineer
Alaska Department of Transportation
and Public Facilities
Fairbanks, Alaska

Douglas J. Goering
Research Engineer
University of Alaska Fairbanks

March 1984

STATE OF ALAKSA
DEPARTMENT OF TRANSPORTATION AND PUBLIC FACILITIES
DIVISION OF PLANNING
2301 Peger Road
Fairbanks, Alaska 99701-6394

in cooperation with

U.S. Department of Transportation
Federal Highway Administration

Technical Report Documentation Page

1. Report No.	2. Government Accession No.	3. Recipient's Catalog No.
FHWA-AK-RD-84-10		

4. Title and Subtitle	5. Report Date
Air Duct Systems for Roadway Stabilization Over Permafrost Areas	March 1984
	6. Performing Organization Code
7. Author(s)	8. Performing Organization Report No.
J. Zarling, B. Connor, D. Goering	FHWA-AK-RD-84-10
9. Performing Organization Name and Address	10. Work Unit No. (TRAIS)
University of Alaska Department of Mechanical Engineering Fairbanks, AK 99701	11. Contract or Grant No. F36192
	13. Type of Report and Period Covered
12. Sponsoring Agency Name and Address	Final
Alaska Department of Transportation and Public Facilities Pouch Z Juneau, AK 99811	14. Sponsoring Agency Code

15. Supplementary Notes

Conducted in cooperation with the U.S. Department of Transportation, Federal Highway Administration

16. Abstract

In the discontinuous permafrost regions of Alaska it is not always possible to route roads over non-permafrost ground. For areas like these, highway engineers face a tremendous design challenge in attempting to provide a stable roadway base. Several active and passive systems have been used in the past to protect the underlying permafrost from thermal degradation. In Alaska, small diameter corrugated metal pipes (culverts) have been placed in the fill material covering the underlying permafrost. Both ends of the culverts are brought to the surface with one end having a long vertical section attached to serve as a stack. Cold air enters the lower end of the culvert, flows through the horizontal section under the roadway cooling the ground (warming the air) and then exits through the vertical stack at the other end of the culvert. Flow is established by the stack or chimney effect, i.e. the warm air is forced up and out of the vertical stack by the heavier surrounding ambient cold air. This report presents the results of both an experimental and analytical research program undertaken to develop design criteria for air duct systems. An experimental duct was assembled and instrumented to determine the relationship between air flow rates and temperature difference, heat transfer rate, air duct length, stack height, etc. A finite element computer model has also been used to investigate the placement of the air duct under the roadway. Optimum design of an air duct system would allow sufficient winter cooling of the ground so that degradation of the underlying permafrost would not occur during the summer thawing season. Temperature contours resulting from the finite element simulations showing the effects of air duct placement on the thermal regime are presented.

17. Key Words	18. Distribution Statement
Permafrost, Air Ducts Heat Flow, Slope Stabilization	N/A

19. Security Classif. (of this report)	20. Security Classif. (of this page)	21. No. of Pages	22. Price
Unclassified	Unclassified	55	N/A

ABSTRACT

In the discontinuous permafrost regions of Alaska it is not always possible to route roads over non-permafrost ground. For areas like these, highway engineers face a tremendous design challenge in attempting to provide a stable roadway base. Several active and passive systems have been used in the past to protect the underlying permafrost from thermal degradation. In Alaska, small diameter corrugated metal pipes (culverts) have been placed in the fill material covering the underlying permafrost. Both ends of the culverts are brought to the surface with one end having a long vertical section attached to serve as a stack. Cold air enters the lower end of the culvert, flows through the horizontal section under the roadway cooling the ground (warming the air) and then exits through the vertical stack at the other end of the culvert. Flow is established by the stack or chimney effect, i.e. the warm air is forced up and out of the vertical stack by the heavier surrounding ambient cold air. This report presents the results of both an experimental and analytical research program undertaken to develop design criteria for air duct systems. An experimental duct was assembled and instrumented to determine the relationship between air flow rates and temperature difference, heat transfer rate, air duct length, stack height, etc. A finite element computer model has also been used to investigate the placement of the air duct under the roadway. Optimum design of an air duct system would allow sufficient winter cooling of the ground so that degradation of the underlying permafrost would not occur during the summer thawing season. Temperature contours resulting from the finite element simulations showing the effects of air duct placement on the thermal regime are presented. From the information presented in this report, the design engineer should find it easier to design air duct systems for roadway stabilization in permafrost areas.

ACKNOWLEDGEMENTS

The authors would like to acknowledge the Federal Highway Administration for their support on this project, under the Highway Planning and Research Program. We also want to acknowledge Allen Braley for his work with the finite element program to produce the roadway section isotherms and Richard Gaffi for setting up the instrumentation on the experimental air duct.

LIST OF FIGURES

LIST OF FIGURES (CONT)

LIST OF TABLES

TABLE OF CONTENTS

Introduction

The existence of permafrost in northern Canada and Alaska has required that those involved in the design of roadways pay special attention to the thermal regime of the ground. In the past, many highway projects have employed varying thicknesses of gravel fill, or in some cases plastic foam board type insulation with gravel fill to thermally protect the underlying frozen ground. However, even if these measures are applied some thawing of the permafrost still occurs, especially in the discontinuous permafrost regions. Depending upon the subsoil type and ice content, this thawing can result in differential settlement leading to costly annual highway maintenance.

The purpose of using gravel fill or using insulation with gravel fill is to maintain the active layer within the non-frost-susceptible fill material. Generally, the thickness of the fill required to thermally protect the underlying permafrost increases as the mean annual soil surface temperature approaches 0°C. The thickness of the fill can be reduced by the use of foam plastic board insulation. However, in discontinuous permafrost zones, this solution may still be cost prohibitive due to the large thicknesses required.

Another common roadway embankment failure in warm permafrost is embankment rotation due to thaw settlement. Even though the embankment's thickness may be sufficient to maintain the permafrost under the snow-cleared roadway, the smaller thickness of gravel in the sideslopes causes this region to experience deeper thawing and continuing thermal degradation of the original permafrost. This degradation can be further accentuated by the sideslopes being insulated with snow, preventing full refreezing during the winter leaving a talik. The thaw settlement which results due to these effects usually shows up as lateral cracking on the wear surface of the roadway, Fig. 1. Typical average annual road surface temperatures are about 32°F while sideslope surface temperatures range from 35° to 40°F.

A potential solution to this problem is the use of ventilated air ducts placed in berm at the toe of the road, Fig. 2. Air duct systems have also been used to stabilize foundations under buildings and tanks, Sanger (1969) and Nixon (1978). These ducts are usually .25 m to .5 m diameter corrugated metal pipe (culvert) with a short sloping or vertical inlet

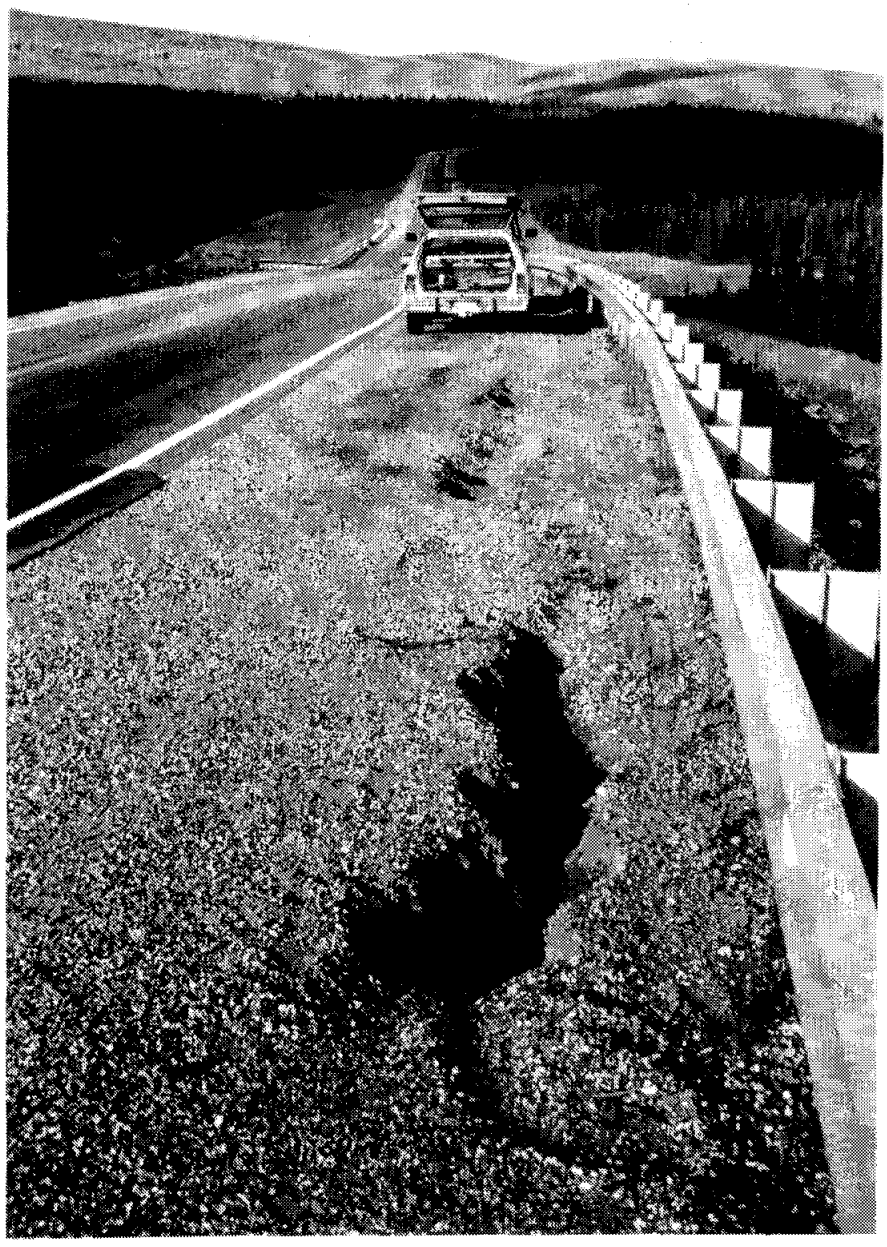

Figure 1: Thaw settlement resulting in lateral cracking.

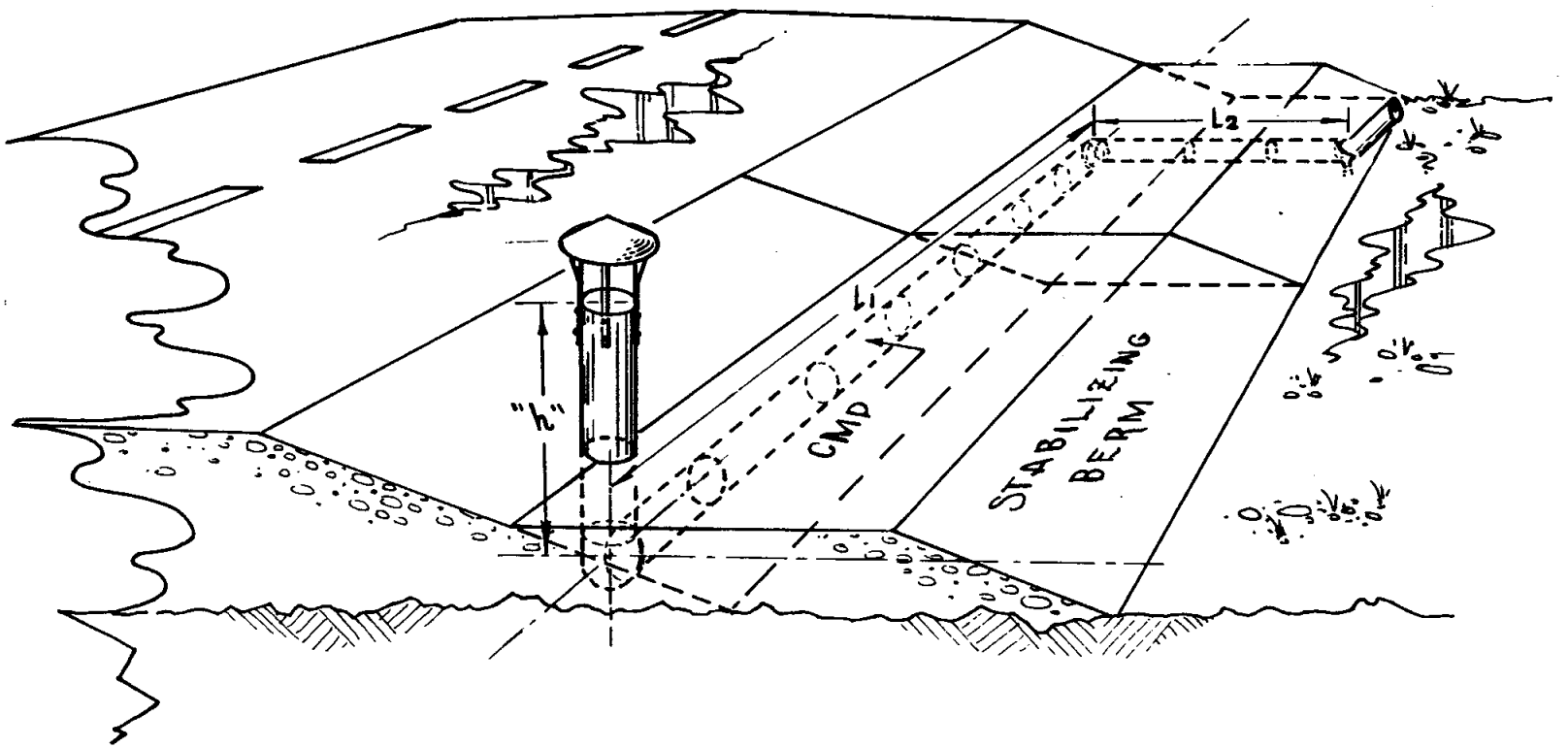

Figure 2: Air duct system.

section leading to a long horizontal section placed in the problem zone connected to a vertical outlet section or stack. Cold air flows in the inlet, is heated by the ground surrounding the buried horizontal section and then flows out the vertical stack. Flow in the duct system is maintained by the "chimney" or "stack" effect. The less dense warm air in the vertical outlet stack is buoyed upward by the surrounding cold ambient air, establishing flow. Flow is maintained as long as the air is heated by the ground, i.e. the ground temperature exceeds the ambient air temperature. During the summer when the ambient air temperature is higher than the ground temperature, flow ceases as the cold air now inside the culvert remains trapped because of its greater density. So, theoretically, the air duct ventilation system is a totally passive device, extracting thermal energy from the ground during the winter accelerating the freeze-back time and then becoming dormant or inoperative during the summer months when thawing from the surface occurs. Wintertime winds will increase the cooling effect (by increased air flow) especially if the inlet and outlet sections have been designed to take advantage of the prevailing wind direction. However, summertime winds can have a detrimental effect if they are allowed to cause flow through the buried ducts.

The remainder of this report will discuss an analytical and experimental effort carried out to investigated the parameters that affect the performance of air duct systems. The hope is that this information will assist the design engineer in optimizing the configuration of these air duct systems. A design methodology is also presented as guidance so the engineer faced with evaluating the potential air duct system as a measure to overcome a potentially sensitive thermal area.

Analysis

A schematic diagram of an air duct system is shown in Fig. 3. The static pressure difference, ΔP_s, created by the stack effect, ASHRAE (1981) is:

$$\Delta P_s = g(\rho_i - \rho_o)h = gh\left(\frac{P_i}{RT_i} - \frac{P_o}{RT_o}\right) \cong \frac{ghP_a}{R}\left(\frac{1}{T_i} - \frac{1}{T_o}\right) \quad [1]$$

where T_i and T_o are the inlet and outlet temperatures, P_a is local atmospheric pressure, and h is the stack height.

If no heating occurs in the inlet section and no cooling occurs in the outlet section, then h in Fig. 3 becomes the effective stack height and ΔP_s can be calculated using equation [1]. This equation shows that a larger temperature difference between the cold and warm air or a longer (taller) stack will increase the stack effect pressure difference resulting in greater air flow. The stack effect pressure difference is balanced by the sum of the velocity pressure P_v and the frictional pressure loss ΔP_f.

$$\Delta P_s = P_v + \Delta P_f. \quad [2]$$

The velocity pressure is

$$P_v = \rho V^2/2 \quad [3]$$

and the friction pressure drop ΔP_f is:

$$\Delta P_f = \rho f L_e V^2/2D \quad [4]$$

The Darcy-Weisbach friction factor, f, in the equation above is determined based on the Reynolds number of the flow within the duct and the relative roughness of the duct. Substituting equations [1], [3], and [4] into equation [2] and rearranging yields an expression for the average air speed in the duct.

$$V = \sqrt{4gh/(1+fL\hat{e}/D)\ [(T\hat{o}-T\hat{i})/(T\hat{o}+T\hat{i})]} \quad [5]$$

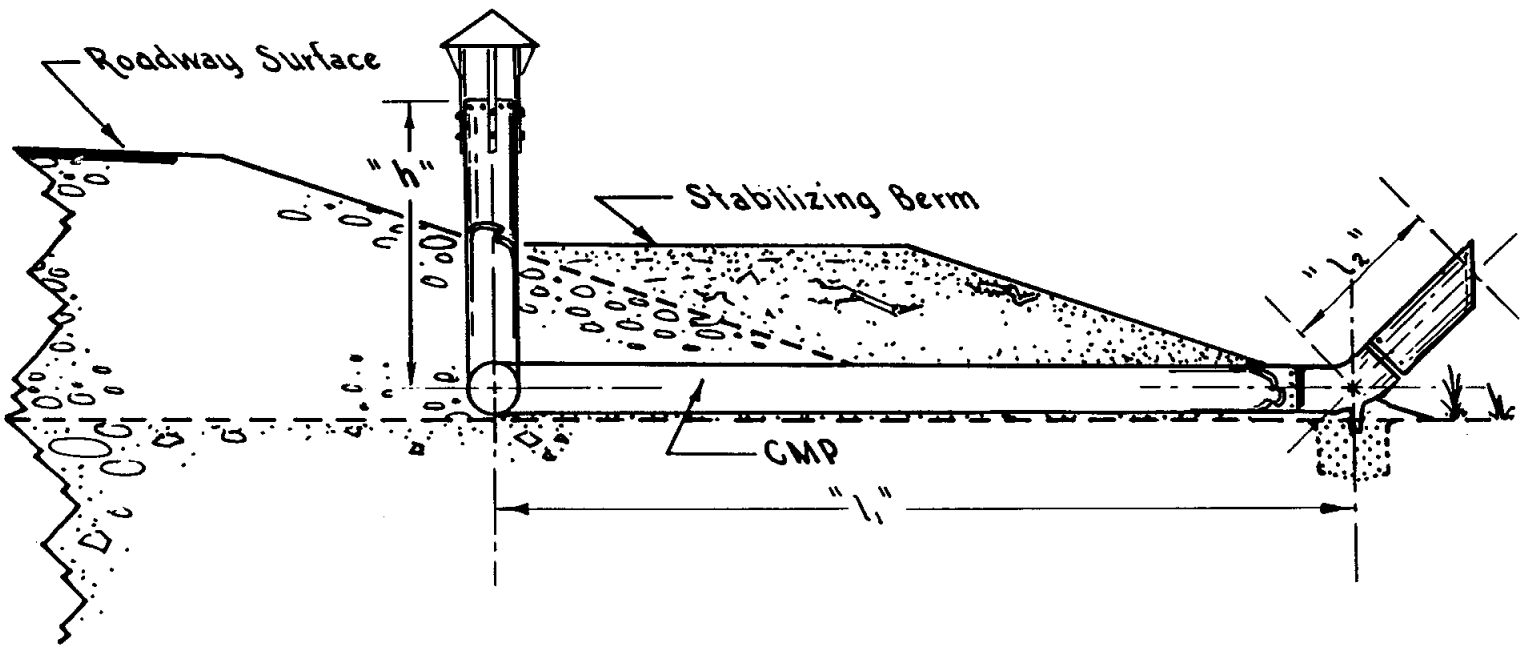

Figure 3: Elevation view of duct.

However, to calculate the duct air speed using equation [5], the friction factor must be known, but the friction factor requires that the Reynolds (air speed) number be specified. Therefore, an iterative method of solution is necessary. It is recommended that a trial value of the friction factor of .08 be used to arrive at a first approximation to the velocity. An improved value of the friction factor can be determined from Fig. 4 once the Reynolds number has been calculated. This iterative process is continued until the desired accuracy is achieved.

If an annular ring of frozen ground of radius R exists around the buried air duct, then the quasi-steady state heat transfer rate to the air flowing through the duct is:

$$Q_t = \frac{(T_f - T_a)}{\frac{1}{h_c \pi D \ell} + \frac{\ln (2R/D)}{2\pi \ell k}} \qquad [6]$$

The heat transfer rate given above is set equal to the thermal energy liberated in the freezing process

$$Q_c = 2\pi R L \ell \frac{dR}{dt} \qquad [7]$$

Equating equations [6] and [7], rearranging and integrating, yields the following relationship:

$$F.I. = L\left\{ \frac{[R^2-(D/2)^2]}{2} \left(\frac{2}{h_c D} - \frac{1}{2k} \right) + \frac{R^2}{2k} \ln (2R/D) \right\} \qquad [8]$$

where F.I. is the freezing index.

This solution neglects the sensible energy changes in the ground and as a result will over-predict the size of the frozen annulus for a given F.I. An improved approximation for the freeze radius that accounts for the non-steady temperature distribution and specific heat effects is given by Harlan (1978) as

$$R' = R(1-.12Ste)^{\frac{1}{2}} \qquad [9]$$

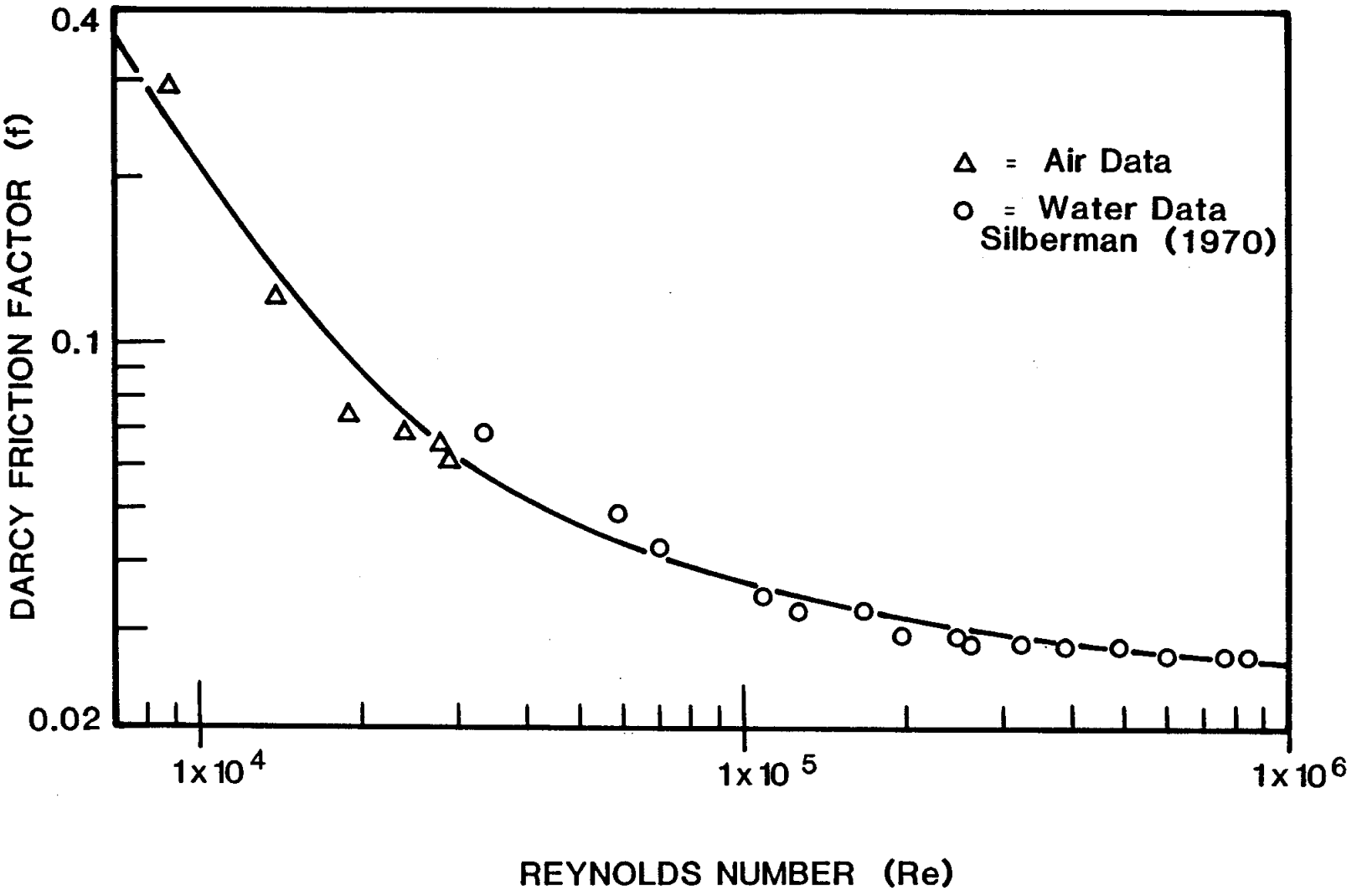

Figure 4: Variation of Darcy Friction Factor with Reynolds Number in a 12-inch diameter helical corrugated metal pipe.

where R is the initial approximation for freeze radius given by equation [8] and R' is the solution of increased accuracy. Ste is the Stefan number defined as the ratio of sensible to latent heat or:

$$Ste = C(T_f - T_a)/L \qquad [10]$$

where C is the volumetric specific heat and $(T_f - T_a)$ is freezing temperature minus the average air temperature in the duct.

Field Installation

In 1973 a research project was initiated under the Highway Planning and Research Program of the Federal Highway Administration to study the benefits of several alternate embankment designs in controlling permafrost thaw under embankment slopes. Insulation, toe berms and air duct sections were installed in 1974 as part of the Parks Highway construction project at Bonanza Creek, approximately 40 kilometers west of Fairbanks.

The roadway embankment was constructed over undisturbed muskeg, underlain by ice-rich silt containing segregated ice. The permafrost temperature was measured to be between -3°C and -1°C. Twenty centimeter diameter galvanized corrugated metal pipe ducts were installed. The inlet ends were placed above the maximum snow cover. The 15 to 30 meter long buried sections were sloped slightly upward toward the 3 meter stack. The conclusions of this study were reported by Esch (1978). Table 1 summarizes the effects of the various treatments.

Table 1 - Maximum Thaw Depths (cm) at Vertical Thermocouple Strings 2.5 meters inside of Normal Embankment Toe, Esch (1978).

	EMBANKMENT DESIGN			
Section Type	1974	1975	1976	1977
Normal Embankment	6 cm	-15 cm	-120 cm	-123 cm
Toe Insulated Embankment	- 6	-24	- 90	-109
3 m Wide Berm	-12	-27	- 75	- 84
6 m Wide Berm	+12	-12	- 45	- 54
6 m Berm & Air Ducts	+24	+ 3	- 36	- 51
Insulated 6 m Berm	+66	+57	+ 39	+ 21
Insulated Berm & Air Ducts	+76	+63	+ 51	+ 39

Air ducts in combination with insulation proved to provide maximum protection against thaw. Air ducts without insulation provided significantly less protection. However, after studying the temperatures along the duct, Esch concluded that the ducts were too long to provide sufficient cooling over their entire length. This claim is substantiated by Fig. 5. As the air flows toward the outlet end, its temperature approaches the ground temperature. Near the outlet of the duct, the temperature differential is quite small resulting in negligible cooling of the surrounding soil. It appears that this duct should have been at least 10 meters shorter.

The heat flow per unit length to this duct can be estimated using the Fourier's Law for radial heat flow, or

$$Q/\ell = \frac{T_o - T_d}{\ln (2R/D)/2\pi k} \qquad [11]$$

The soil density at the site is approximately 1600 kg/m^3 with a 15% moisture content by weight and a thermal conductivity of 1.5 W/m °C. Using the pipe radius, D/2, as 0.10 m (thermal couple string No. 1) and the outer soil radius, R, of 0.40 m (thermal couple string No. 2), the heat flow per unit length at any point along the duct can then be calculated using equation [11]. The heat transfer rate along the pipe for January 1980 is plotted in Fig. 6. The total energy transferred can be calculated by integrating the heat transfer rate per unit length over the entire length of air duct or,

$$Q_t = \int (Q/\ell)\, dx = 381.1 \text{ W}$$

From the First Law of Thermodynamics, the energy transferred to the air flowing through the duct is

$$Q_t = m\, c_p \Delta T \qquad [12]$$

where the mass flow rate, m, in the above equation can be expressed as

$$m = A\rho V \qquad [13]$$

Substituting equation [13] into equation [12] and rearranging yields

$$V = Q_t/A\rho c_p \Delta T \qquad [14]$$

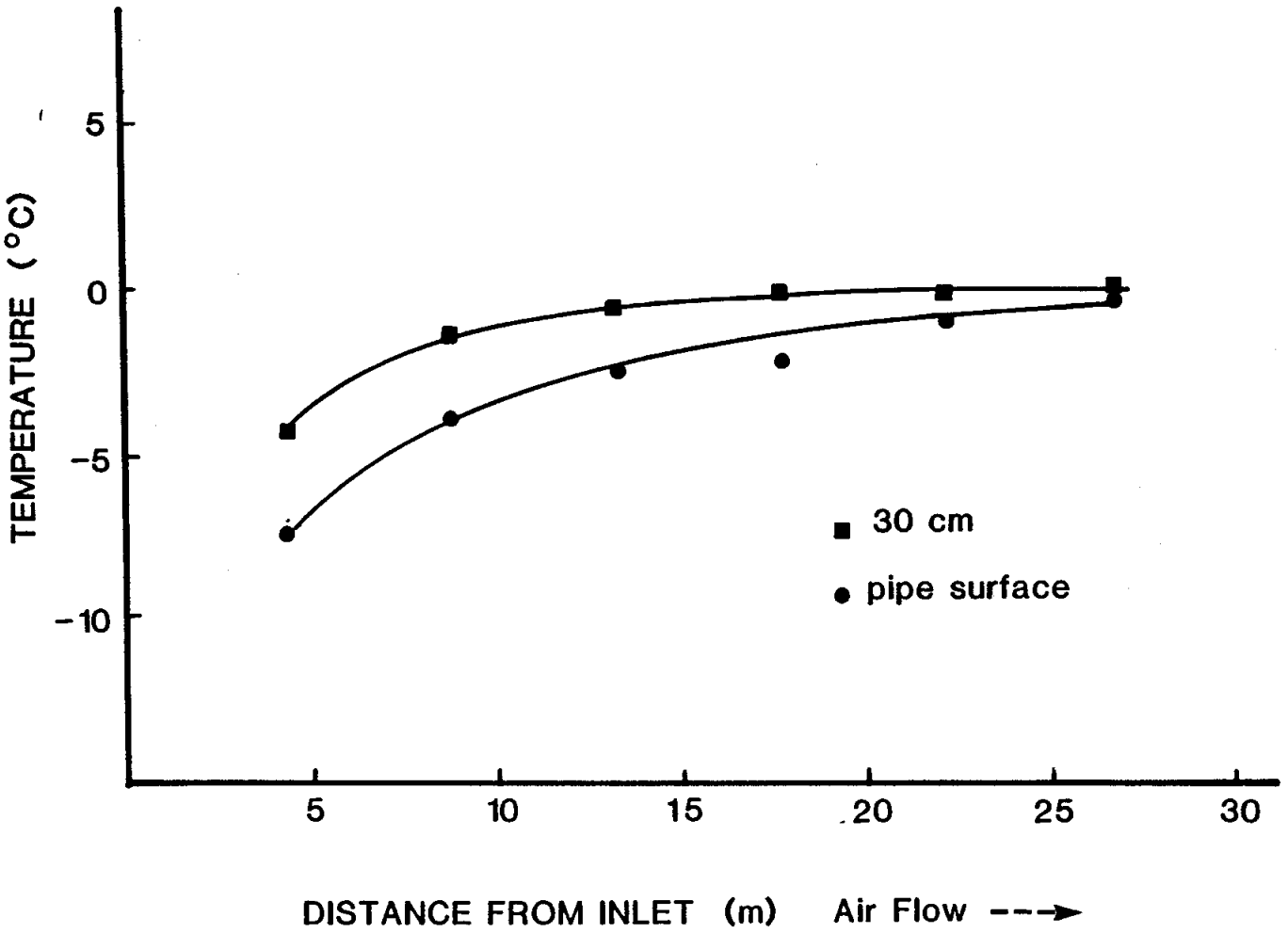

Figure 5: Temperature of pipe surface and 30 cm from pipe surface at Bonanza Creek, January 1980.

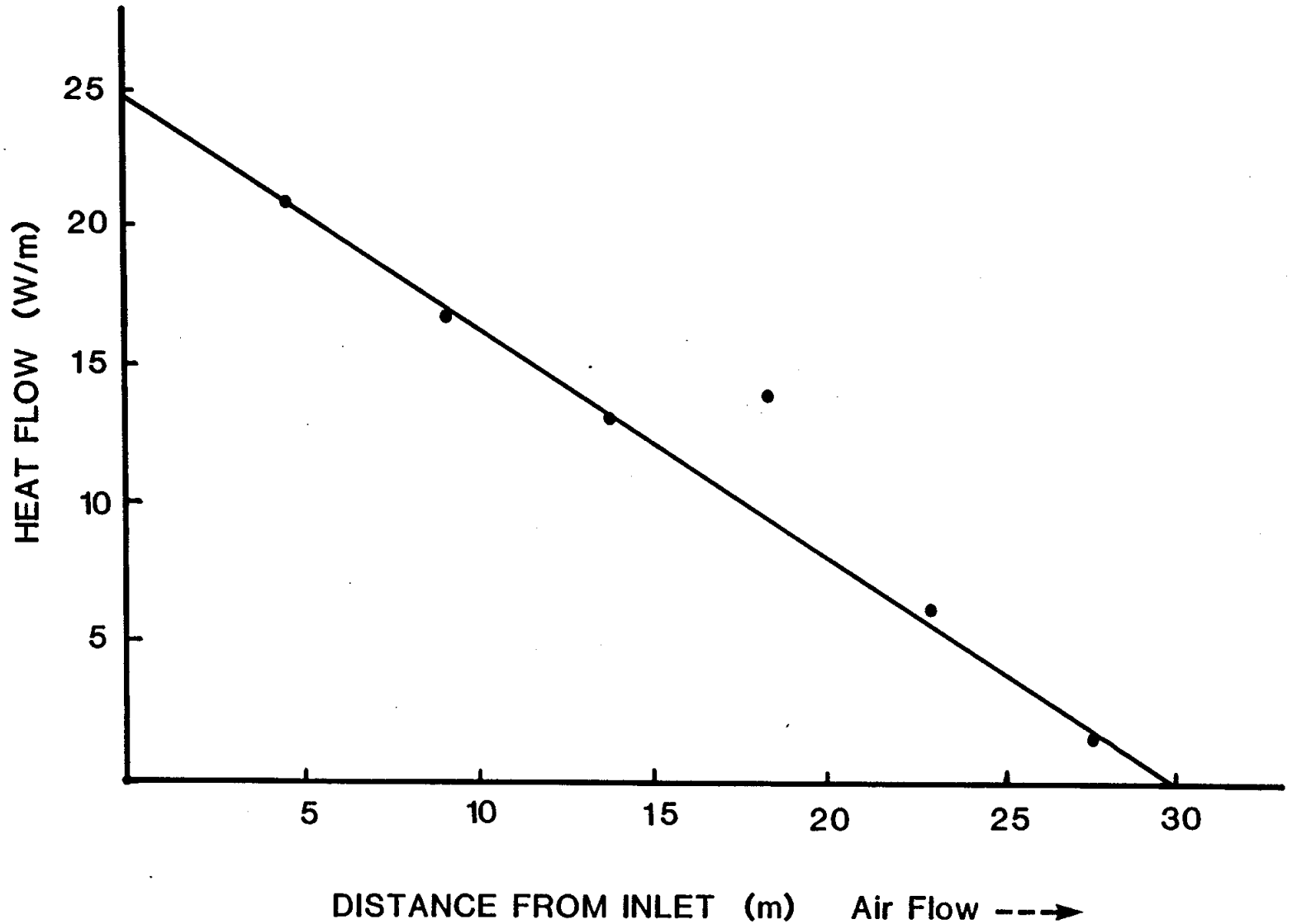

Figure 6: Heat flow from duct, January 1980.

Using the thermal properties of air at 0°C and the Q_t value given above, yields an air speed in the duct at

$$V = 0.33 \text{ m/s}$$

Field measurements have indicated approximate air speed of 0.3 m/s at a ΔT of 30°C.

Computer Modeling

The air duct system was modeled on the University of Alaska Computer Network (UACN) Honeywell Computer using the DOW Chemical Model, "Finite Element Heat Conduction Program", Wang (1979). The model is designed to solve a two dimensional heat conduction problem, assuming there is no temperature gradient in the third direction. Boundary temperatures may be either fixed or time-varying. Each nodal point can be either a heat source or a heat sink.

The program further assumes that phase change occurs between 0°C and -1°C. Latent and sensible heats have been combined for this region to yield an apparent specific heat. (Most fine grained soils exhibit some subcooling in the freeze-thaw process as well as latent heat being liberated over a temperature range due to unfrozen water content). The thermal conductivity of the soil can be varied in the x and y directions and was assumed uniform for the same soil type but varied from layer to layer.

The air duct system placed in the embankment is shown in Fig. 7. The embankment is comprised of three layers with the duct positioned at the surface of the original ground. The properties of each layer are indicated on Fig. 7. A 0.6 meter snow cover was placed on the embankment slopes and the berm between October 1 and April 15 of each year. The pavement surface was left bare throughout the year. The surface temperature was modeled by the cosine function:

$$T_s = \bar{T}_s - T_v \cos (wt - w\phi) \qquad [15]$$

Subgrade Material	Density kg/m³	Moisture % by wt.	Thermal Conductivity w/m°K	
			Frozen	Thawed
Crushed Gravel	2200	6%	3.114	2.768
Gravel	1600	20%	2.768	1.903
Permafrost	1200	40%	2.076	1.038
Organic Silt	1200	10%	0.606	0.571

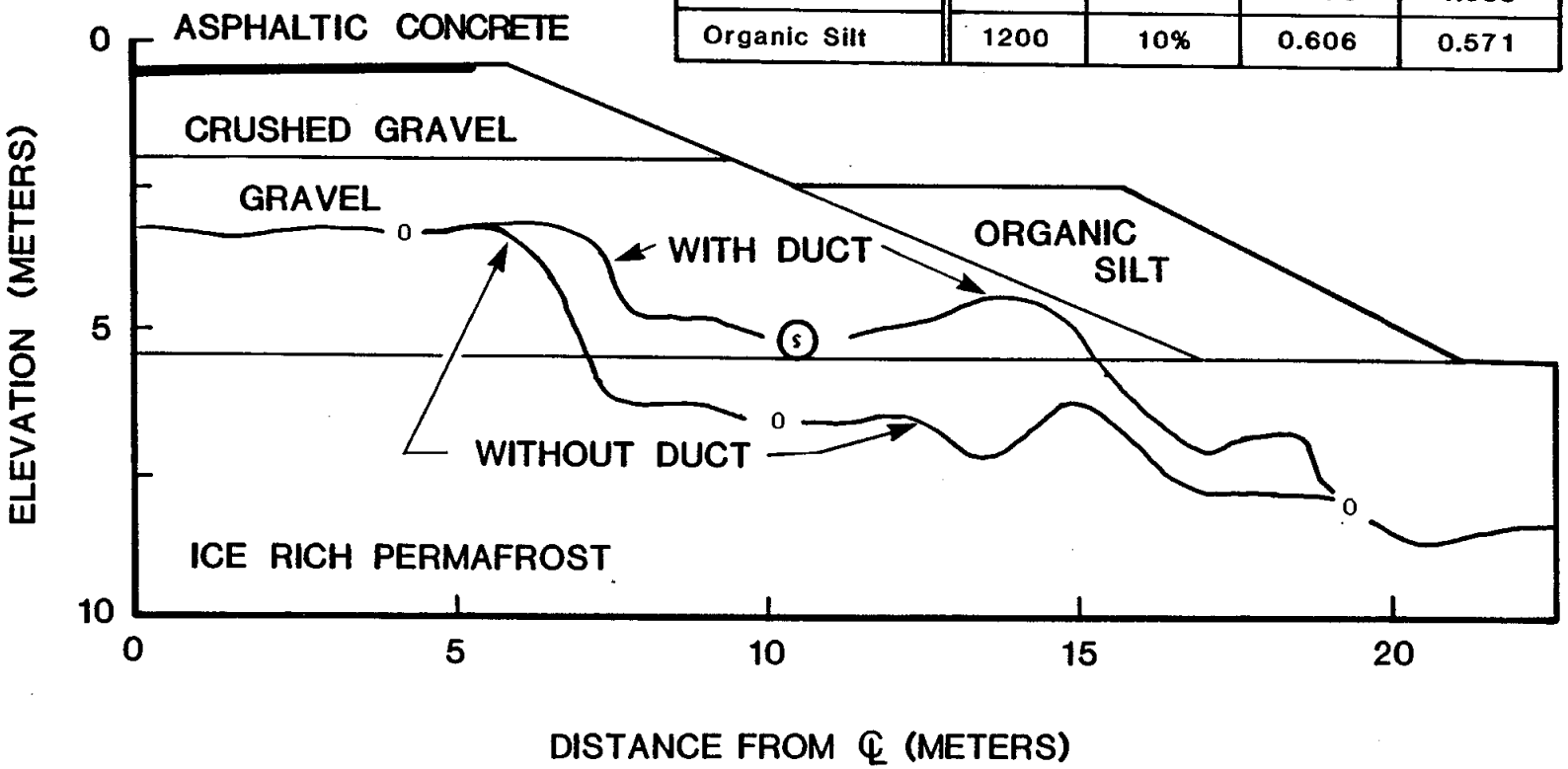

Figure 7: Finite element simulation of duct in August.

The following values were used;

$$\bar{T}_s = -3°C,\ T_v = 20°C,\ \text{and}\ \phi = 10\ \text{days}.$$

An initial run was made without the duct to determine the thermal effect of the embankment on the underlying permafrost. As might be expected, degradation of the permafrost was noted beneath the shoulder and would be evidenced on the pavement surface as a longitudinal cracking. Additional runs were made with the air duct using a convective heat transfer coefficient of 9.7W/m²-°C for the pipe and an air temperature equal to outdoor ambient. As seen in Fig. 7, the use of the duct raised the 0°C isotherm into the embankment, thereby preserving the permafrost.

It should be noted that the computer model provides an upper bound to the field installation thermal regime. The duct in the model was larger and placed more effectively under the embankment in comparison to the Bonanza Creek installation. Ideally, the duct should be placed far enough under the embankment to prevent the degradation of permafrost beneath the shoulder material. Appendix A contains the isotherms for several duct placement variations for the months of March and September.

Experimental System

An experimental facility was constructed during 1982 in order to augment field data obtained at Bonanza Creek. The experimental facility, Fig. 8, consisted of the air duct, an adjustable electric heating circuit, and data acquisition system. Helically corrugated metal culvert 30 cm in diameter (60 cm plate and 7 x 1.5 cm corrugations) was used for construction of the air duct. The horizontal section was 12.5 meters in length with a one meter vertical inlet section and a vertical outlet stack of variable length. Heat input was accomplished via copper clad heating tapes wrapped in the corrugations on the outside of the duct. Three separate heating circuits spanning the horizontal section of the duct were employed as shown in Fig. 9. In order to reduce heat transfer directly to the outside air and to maintain a stable duct temperature, 5 cm of fiberglass insulation were wrapped around the outside of the horizontal section covering both the duct and heating coils.

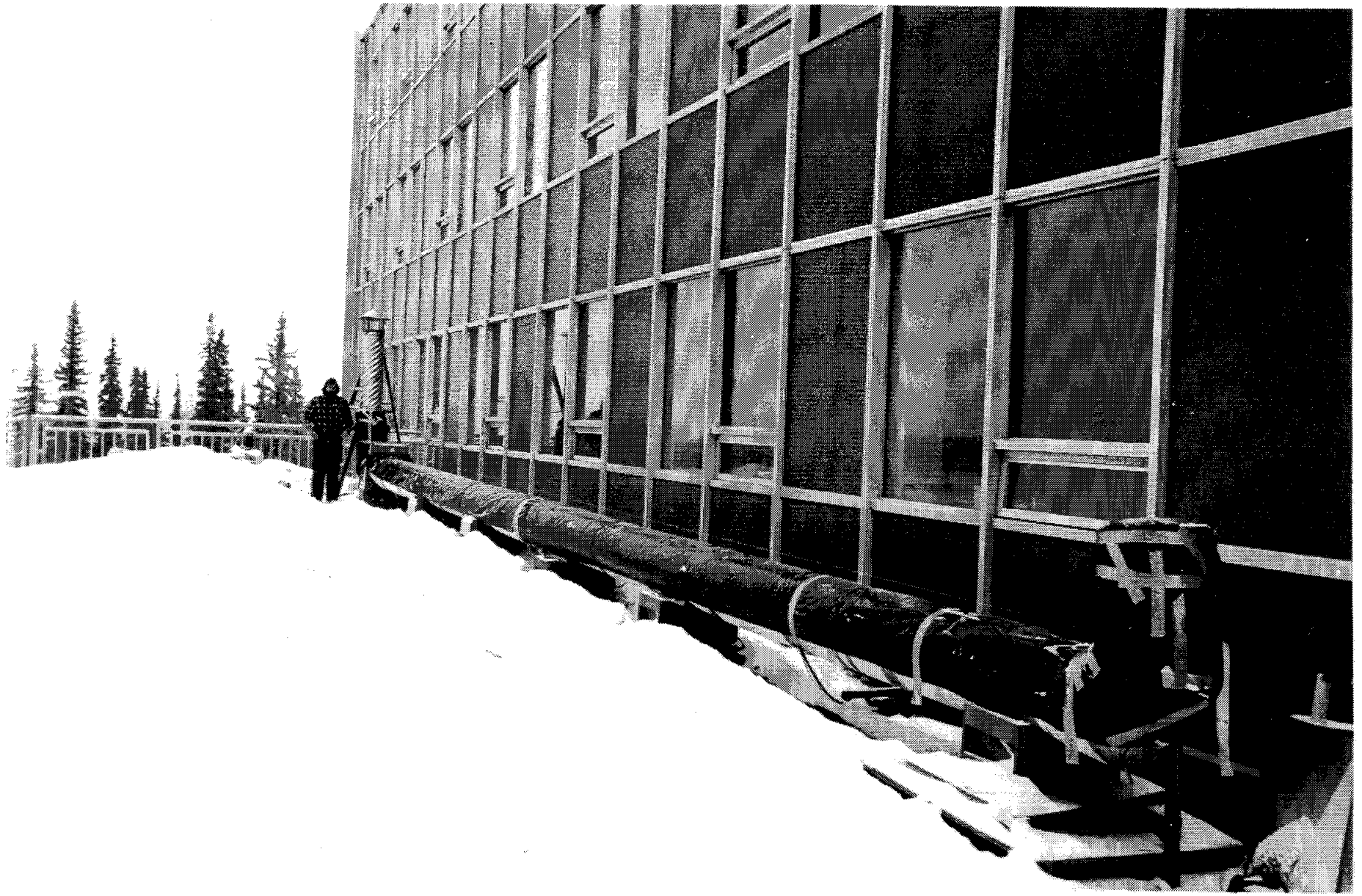

Figure 8: View of air duct system used for roadway stabilization.

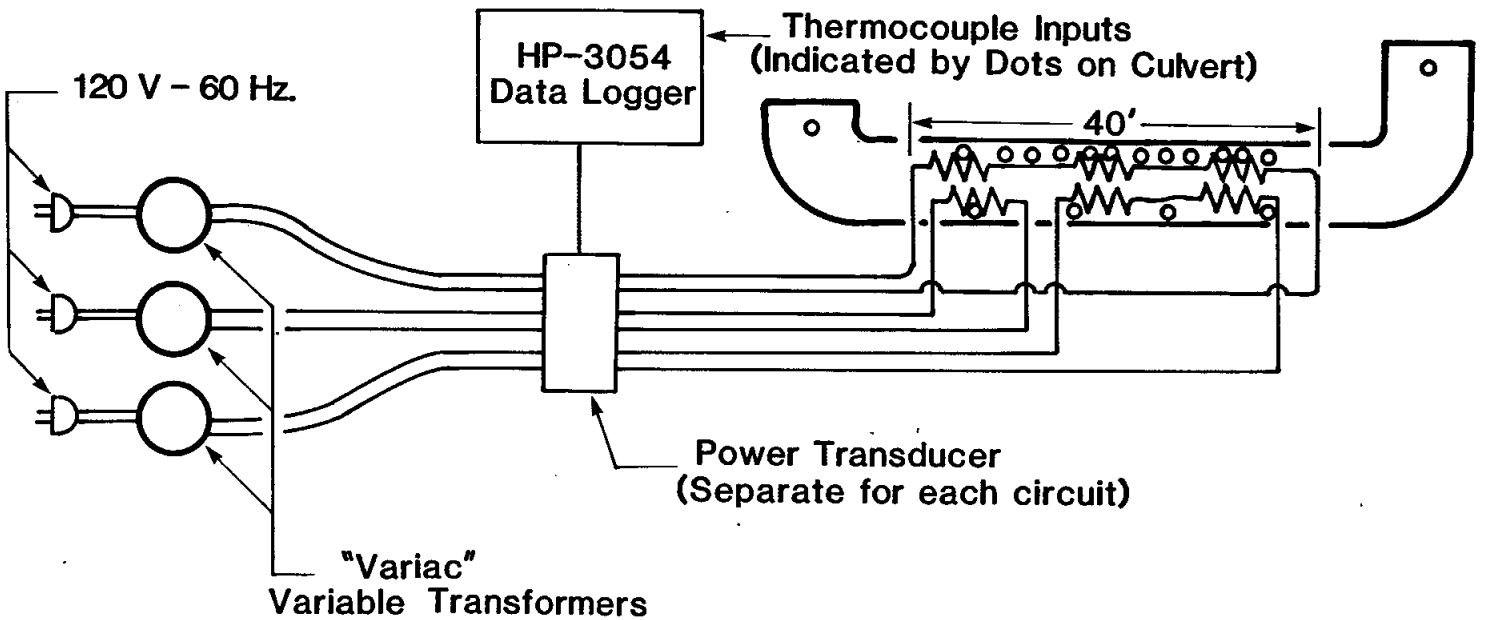

Figure 9: Schematic of experimental air duct.

Each of the coils was powered by a "Variac" variable transformer and monitored by an individual power transducer. This allowed for flexibility not only in overall heat input but also in the heating profile along the duct. Thermocouples were used to measure both air temperatures within the duct, and temperatures of the duct surface. Temperature and heat input data were collected with a Hewlett-Packard 3054A data acquisition system. The 3054A system consists of an HP-85 computer which is interfaced to a 3497A data acquisition/control unit which is in turn interfaced with the power transducers and temperature probes.

Headloss-flowrate tests were run on a 12.5 m horizontal section of the 30 cm diameter duct. Pressure drop data at flowrates covering Reynolds numbers from 7,000 to 30,000 were recorded. Darcy-Weisbach friction factors were calculated from the data and the results have been plotted in Fig. 4. Data from tests conducted with water in 30 cm diameter helical culverts by Silberman (1970) is also shown in this figure.

A series of thermal performance tests were conducted as outlined in Table 2.

Table 2 - Experimental Tests--Duct Configurations

No.	Stack Heights	Duct Configurations
1	2. 1 m	no stack insulation, no weather caps
2	3.35 m	no stack insulation, no weather caps
3	4. 6 m	no stack insulation, no weather caps
4	3.35 m	no stack insulation, weather caps installed
5	3.35 m	stack insulated, no weather caps

Experiments 1, 2, and 3 investigated the effect of outlet stack length on duct operation. Experiment 4 concerned the effect of placing weather caps as seen in Fig. 8 on the inlet and outlet openings, and 5 dealt with insulation on the outlet stack. Each of the experiments was run for six twenty-four hour periods at different power input levels. Temperatures and power inputs were scanned and recorded hourly during each period.

Reduction of the recorded data was accomplished by inspecting it for periods of stable operation. Usually a stable outside air temperature

resulted in stable duct operation although this was not always the case, particularly during windy weather. In general, one twenty-four hour period resulted in three or four usable scans.

Analysis proceeded with the calculation of the amount of thermal energy transferred to the air inside the duct. This was achieved by subtracting the heat lost through the insulation directly to the outside air from the total heat input recorded by the data logger.

$$Q_{air} = Q_{tot} - Q_{lost} \qquad [16]$$

A value for the thermal resistance of the insulating layer covering the heat tapes and duct was obtained by heating the duct with airtight, insulating covers at the inlet and outlet ends. In this situation all power input by the heat tapes must escape through the insulation. Consequently, a thermal resistance value can be calculated simply by noting the heat input and the temperature drop across the layer. Once this resistance is known it is possible to calculate the amount of heat being transferred to the air flowing through the duct as described above. This value can then be used in conjunction with inlet and outlet duct air temperatures to calculate the mass flow rate of duct air, Reynolds number, and the convection heat transfer coefficient using the equations given below.

$$\begin{aligned} m &= Q_{air}/c_p\Delta T \\ Re &= mD/A\mu \\ h_c &= Q_{air}/A_s(T_d-T_a) \end{aligned} \qquad [17]$$

Finally, the experimental results are presented as plots of m versus Q_{air} and h_c versus Reynolds number.

Experimental results presented here were obtained during the fall and winter of 1982 on the University of Alaska-Fairbanks campus. Outside air temperatures ranged from -5°C to -43°C. The heating circuits were adjusted to deliver a uniform heat flux along the entire horizontal section of the duct. Initial experimentation was hampered by difficulty in establishing proper air flow in the duct. By introducing a 1.5% slope to the horizontal section with the outlet at the high end, this problem was eliminated.

Results are shown in Figs. 10-12. As expected a taller stack results in a larger draft head which in turn produces larger mass flow rates, Fig. 10. Figure 11 shows the effect of insulating the outlet stack with 5 cm of paper faced fiberglass. This figure shows that such insulation has a detrimental effect on duct operation and is backed-up, at least in part, by field observations conducted at Bonanza Creek. Figure 12 is a plot of h_c versus Re with data from all five experiments included. Theoretical h_c values calculated using the Reynolds analogy relating fluid friction and heat transfer were in good agreement with Figure 12. Results obtained for duct operation with weather caps on the inlet and outlet openings revealed reductions in mass flow rates of up to 20%. The weather caps used in this experiment were of the inverted cone type with a 15 cm gap between the cone and duct opening. This effect will vary depending on the geometry of the cap installation; therefore results have not been presented graphically. Finally, stack efficiencies have been calculated by dividing the theoretical velocity given in [5] by the observed velocities. An average efficiency of 90% was obtained with a standard deviation of 3.5%.

Originally it was expected that insulating the outlet stack would improve duct performance by maintaining a higher air temperature in the stack and thereby increasing the draft head. As mentioned above however, the opposite was found to be the case. A possible explanation is that when no insulation is present on the outlet stack the stack itself will have a relatively low temperature, consequently the air film on the inside surface will be at a lower temperature and therefore lower viscosity. On the other hand, with insulation on the outside of the stack, a higher surface temperature results in a more viscous air film on the inside surface of the stack. Therefore, insulating the stack results in higher frictional losses in the stack which may be substantial enough to overshadow the increases in the draft head.

Design Procedure

A design procedure can be developed based on the information presented in this paper. If a talik of radius R needs to be frozen back, then equations [8] and [9] can be used to determine the required freezing

Figure 10: Effect of stack height.

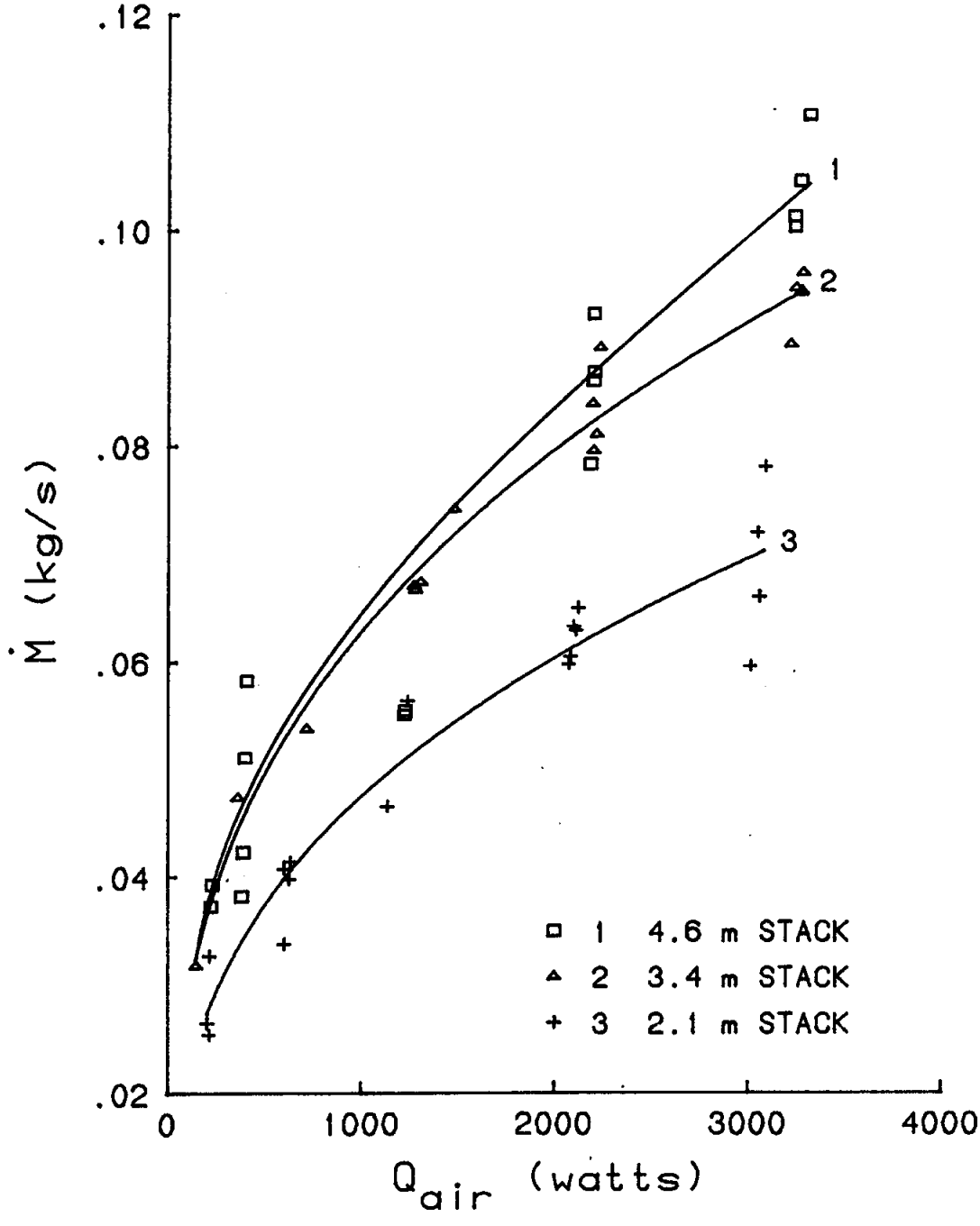

Figure 11: Effect of stack insulation.

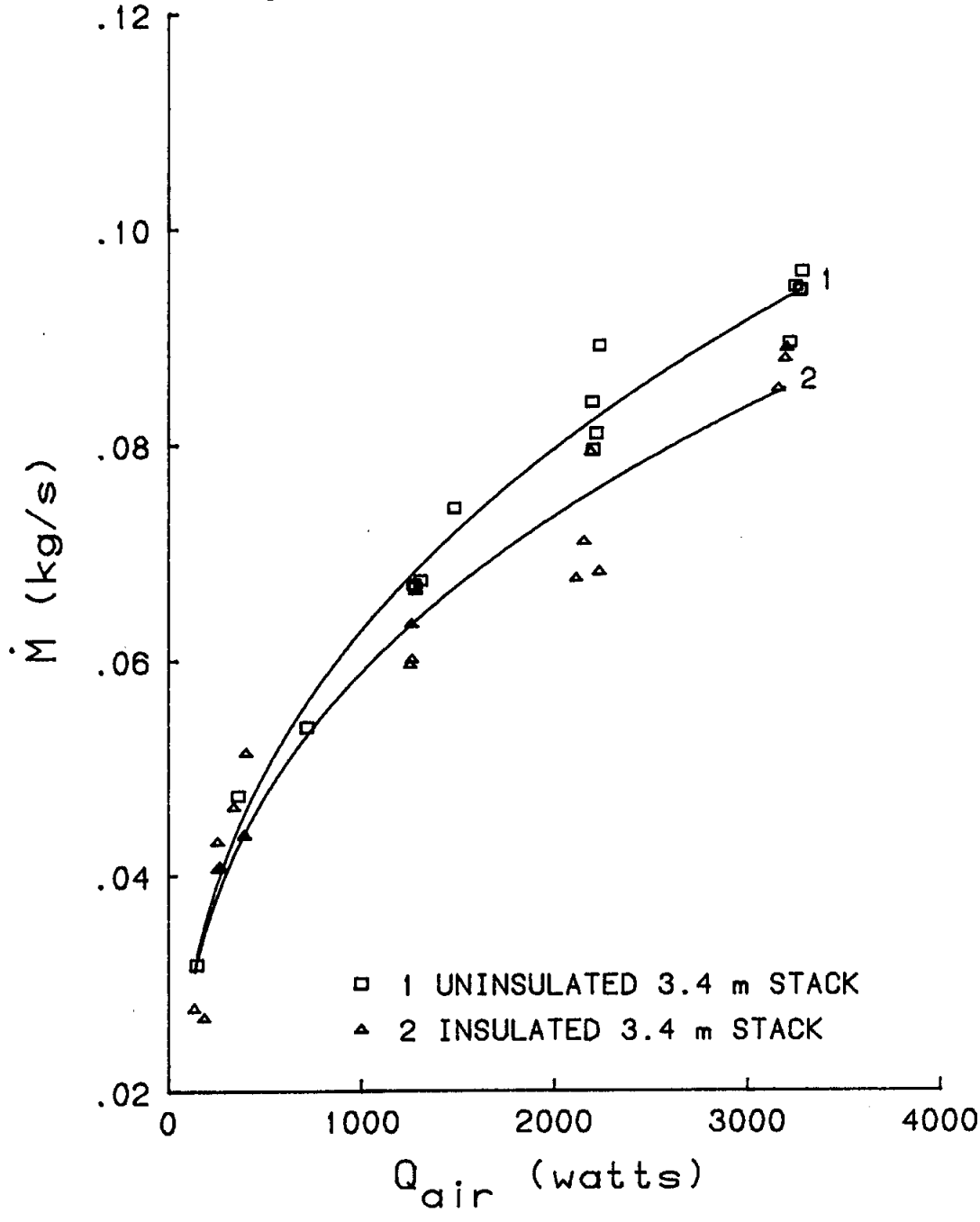

Figure 12: Heat transfer coefficient ($\widehat{hc}$).

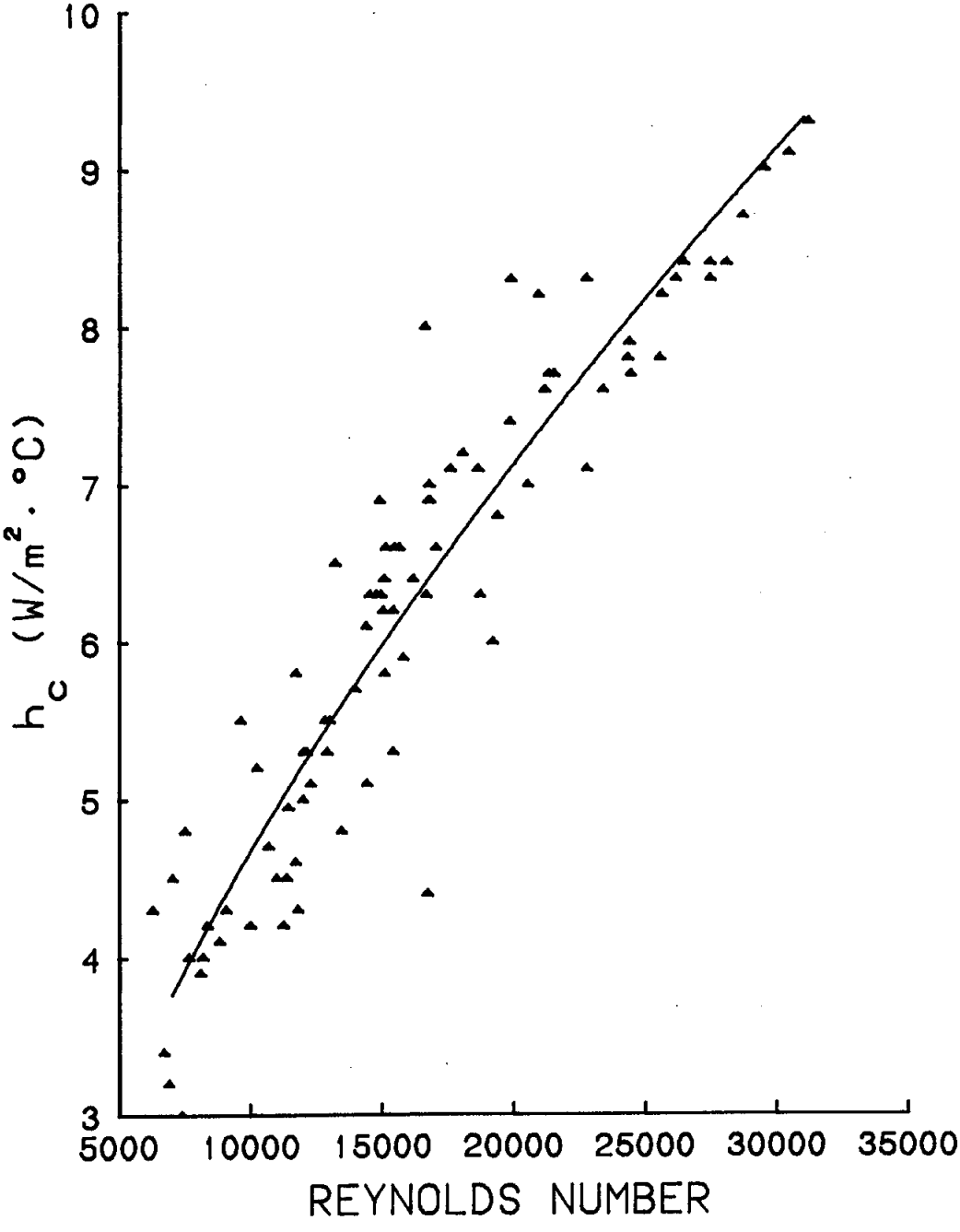

index. Figure 12 would be used to choose an appropriate convective heat transfer coefficient. If this freezing index was less than the air freezing index for the site then a dual air duct system should be considered. Next, the maximum permissible temperature leaving the stack can be calculated by dividing the freezing index from equation [8] by the length of the freezing season. The total energy removed from the ground can be estimated by determining the heat transfered in freezing and sensibly cooling a talik of effective radius R'. The average heat removal rate is found by dividing the total energy removed by the length of the freezing season. Then the average air speed in the duct can be calculated by equation [14]. The equivalent length of air duct is then calculated using equation [5] with the appropriate friction factor taken from Figure 4 and the stack height assumed. Finally, the length of the buried section is calculated by subtracting the inlet length, outlet length, and fitting losses from the equivalent length.

DESIGN CALCULATION METHODOLOGY

The design calculation methodology is presented in English Engineering Units in the belief that highway engineers still favor this system.

Step 1

Determine the climatic conditions at the site. The Environmental Atlas of Alaska, Hartman and Johnson (1978), contains the following required data:

A.T.I. --- air thawing index, °F-Day
A.F.I. --- air freezing index, °F-Day
Tm --- mean annual air temperature. °F

Step 2

Determine the soil conditions at the site. The required geotechnical data is soil types, dry densities and moisture contents. Calculate the volumetric specific and latent heats of the soils.

$L = 1.44\rho_D W$, Btu/Ft^3 volumetric latent heat

$C_t = \rho_D(.18 + .010W)$, $Btu/Ft^3\text{-}°F$ volumetric specific heat--thawed

$C_f = \rho_D(.18 + .005W)$, $Btu/Ft^3\text{-}°F$ volumetric specific heat--frozen

The thermal conductivities of soils based on dry densities and moisture contents are given in graphical form in Sanger (1963).

Step 3

Estimate the radius of the talik that would be formed in the roadway embankment without an air duct device. Appendix A contains several thermal contour plots for different surface conditions that can be used as guidance in making this estimate. Calculate the freezing index required to freeze-back this talik using equation [8]. As a first approximation, use a value of h_c equal to 2 $Btu/Hr\text{-}Ft^2\text{-}°F$. If the required freezing index is greater than the air freezing index, consider using two air ducts placed in parallel.

Step 4

Determine the average air temperature, T_{ad}, leaving the air duct based on the required freezing index calculated in Step 3. t_f is the length of the freezing season based on the air freezing index taken from Sanger (1963).

$\Delta T_{ad} = F.I./t_f$

$T_{ad} = T_f - \Delta T_{ad}$

Step 5

Calculate the average air temperature, T_{ed}, entering the air duct based on the site air freezing index and the length of the freezing season, Sanger (1963).

$$\Delta T_{ed} = A.F.I./t_f$$

$$T_{ed} = T_f - \Delta T_{ed}$$

Step 6

Correct the talik radius used in equation [8], step 3 using equation [9]. Calculate the Stefan number, equation [10], using ΔT_{ad} and ΔT_{ed}.

$$R' = R/(1-.12Ste)^{\frac{1}{2}}$$

Recalculate the required freeze index and mean air temperature leaving the air duct using R' for R.

Step 7

Calculate the total energy removed from the talik to freeze it back,

$$Q' = \pi[R'^2 - (D/2)^2]\, L\ell$$

where ℓ is the estimated length of the buried portion of the air duct.

Step 8

Calculate the minimum required average air speed in the air duct using equation [14]. ΔT is the average inlet-outlet temperature difference.

$$\Delta T = T_{ad} - T_{ed}$$

Step 9

Solve equation [5] for the theoretical average air speed in the air duct based on the equivalent length of the air duct. The total equivalent length is calculated by adding the equivalent length of the elbows, the inlet length and the vertical outlet length to the length of the buried section. Equation [5] should be corrected with a chimney efficiency factor of 90% which reduces the air speed calculated by 10%. If the actual average air speed is less than that calculated in Step 8, either extend the length of the vertical outlet stack, enlarge the duct diameter, or shorten the length of the buried horizontal section.

Step 10

Calculate the Reynolds number of the flow and check the accuracy of estimated heat transfer coefficient, Figure 9, and Darcy Friction Factor Figure 2. Redo calculations using improved values of these parameters.

Sample Calculation

A talik 3 feet in radius is to be frozen-back in the Fairbanks, Alaska area using a 1 foot in diameter corrugated metal pipe air duct. Soil conditions at the site are silts with a dry density of 100 lb/Ft^3 and average moisture contents of 10%.

Step 1

From the Environmental Atlas of Alaska, the site climatic data are:

A.T.I. = 3,000 °F-days

A.F.I. = 5,500 °F-days

Tm = 25°F

Step 2

The soil thermal properties are:

$L = 1.44\rho_D W = 1.44(100)(10) = 1{,}440$ Btu/Ft³

$C_t = \rho_D(.18 + .01W) = 100\ [(.18 + .01(10)] = 28$ Btu/Ft³-°F

$C_f = \rho_D(.18 + .005W) = 100\ [(.18 + .005(10)] = 23$ Btu/Ft³-°F

$k_t = .6$ Btu/Hr-Ft-°F

$k_f = .6$ Btu/Hr-Ft-°F

Step 3

Talik radius given at 3 feet. Assume h_c equals 2 Btu/Hr-Ft²-F, calculate the required freezing index using equation [8]

$$F.I. = L\{[R^2 - (D/2)^2]\ [1/(h_cD)-1/(4K)] + R^2\ln(2R/D)/(2K)\}$$

$$F.I. = 1{,}440\ \{[9-.25]\ [1/(2.0)\ -1/(2.4)] + 9\ln(6.0/1.0)/(1.2)\}$$

= 20,400 F-Hrs = 850 F-days

Step 4

The length of the freezing season, t_f, is 210 days, Sanger (1963). The maximum average air temperature leaving the duct is

$$\Delta T_{ad} = F.I./t_f = 850/210 = 4°F$$

$$T_{ad} = 32 - 4 = 28°F$$

Step 5

The average air temperature entering the duct is

$$\Delta T_{ed} = A.F.I./t_f = (5,500)/210 = 26°F$$

$$T_{ed} = 32 - 26 = 6°F$$

Step 6

The Stefan number leaving duct:

$$Ste = C_f \Delta T_{ed}/L = (23)(4)/1,440 = .06$$

The Stefan number entering duct:

$$Ste = C_f \Delta T_{ad}/L = (23)(26)/1,440 = .42$$

Average Stefan number is .24

Calculate the effective talik radius including specific heat effect:

$$R' = R/(1-.12\ Ste)^{\frac{1}{2}}$$

$$R' = 3/[1-.12(.24)]^{\frac{1}{2}} = 3.04 \text{ feet}$$

Using equation [6], calculate new freexing index required and air temperature leaving duct.

F.I. = 21,200 F-Hrs = 882 F-days

ΔT_{ad} = 882/210 = 4F

T_{ad} = 32-4 = 28F

Step 7

Calculate total energy removed from talik:

$Q' = \pi[R^2-(D/2)^2]\,\ell L = \pi[3.04^2-.5^2]\ell(1,440) = 40,700\,\ell$ Btu

Step 8

Calculate minimum air speed

$V = Q'/\rho Ac_\rho \Delta Tt_f = 40,700\ell/(.083)(.25\pi)(.24)(28-6)(210)(24)$

= 23.5ℓFeet/Hour
= .007ℓFeet/Sec

Assume ℓ is 100 feet, then

V = .7 Feet/Sec

Step 9

Assume an entrance length of 10 feet at a 45 angle and a vertical stack of 20 feet. The loss coefficients, ASHRAE (1981) are:

	Loss Coefficient
Sharp Edge Entrance	K = 1.0
45 Miter Elbow	K = .48 Re = 10,000 K = .43 Re = 20,000
90 3 Piece Miter Elbow	K = .59 Re = 10,000 K = .53 Re = 20,000
90 2 Piece Miter Elbow	K = 1.7 Re = 10,000 K = 1.5 Re = 20,000

To calculate the equivalent length of the fittings,

$$L_e/D = \Sigma K/f$$

Assuming a 45 Miter Elbow at the inlet end and a 3-piece 90 Miter Elbow at the outlet end will be used, then:

$$L_e/D = (1.0 + .43 + .53)/.09 = 22$$

where the friction factor, f, was chosen at .09 at a Reynolds number of 20,000, Figure 2. Then, the total equivalent length is:

$$L_e = 10 + 100 + 20 + 22 = 152 \text{ Feet}$$

Inlet Duct + Horizontal Duct + Stack + Minor losses

The theoretical air speed in the duct given by equation [3] is

$$V_t = \{[4gh/(1+L_e/D)]\ [(T_{ad} - T_{ed})/(T_{ad}+T_{ed})]\}^{\frac{1}{2}}$$

$$V_t = \{[4(32.2)(20)/(1+.09(152)/1)]\ [(488-466)/(488+466)]\}$$

where T_{ad} = 460 + 28 = 488 R and T_{ed} = 460 + 6 = 466R

$$V_t = 2.01 \text{ feet/sec}$$

This theoretical value of the air speed must be reduced by 10% for stack efficiency, or

$$V_a = eV_t = .9(2.01) = 1.8 \text{ feet/sec}$$

The actual air speed of 1.8 feet/sec is greater than the required air speed of .7 feet/sec, so duct should work.

Step 10

Check Reynolds Number,

$$R_v = VD/\upsilon = (1.80)(1.0)/12X10^{-5} = 15{,}000$$

From Figure 2, f = .11 and from Figure 9, h_c = 1.20 Btu/Hr-Ft²-°F. Redo calculations starting at Step 9 using these new values yields an actual air speed of 1.6 feet/second. A second iteration yields an actual air speed of 1.5 feet/second. The system still works. (In fact, the stack height could be shortened or horizontal section lengthened.)

Summary and Conclusions

Highway designers in Alaska have traditionally had few tools to combat degradation of permafrost beneath embankments. Several active and passive devices have been used in recent years to protect underlying permafrost from thermal degradation. While insulation has proven successful in reducing embankment thickness, it has proven ineffective in protecting the permafrost beneath the embankment sideslopes. This results in longitudinal cracking in the roadway surface.

A system of air ducts were installed on the Parks Highway at Bonanza Creek approximately 40 kilometers west of Fairbanks in 1974. However, no design methodology was available at that time to size the system. Consequently, the system was too small to provide long term thermal stability.

This report provides a design procedure by which the system can be sized to insure the zone beneath the sideslopes remains frozen. The development of the design methodology has necessitated the determination of friction factors for low velocity air through a corrugated metal pipe, heat transfer coefficents, relationships between stack height and air velocity etc. These parameters have been determined and reported here.

The optimum location of the air duct system has also been determined. Ideally, the system should be placed in the center of the thaw bulb or talik beneath the embankment sideslopes. This can be estimated using the information in Appendix A. The center of the thaw zone can also be computed using one of several computer modeling systems presently available. This will generally give a better prediction of the size of the talik for the particular environment in question than Appendix A.

In conclusion, the design procedure given here allows the design engineer to properly size an air duct system to meet a particular application.

Implementation

Theoretical analysis shows the use of air ducts can greatly reduce or eliminate shoulder rotation above thaw sensitive permafrost. A system of air ducts was installed at approximately mile 1240 on the Alaska Highway near the Canadian Border. This installation was heavily instrumented to provide a check for the design procedure developed under this project.

Air duct stabilization systems should be considered whenever embankment shoulder rotation is expected. The design methodology developed and reported here should be used to size the system to meet site requirements. While current costs seem high, as contractors become more familiar with such systems, the costs will be reduced.

It is therefore recommended that whenever air ducts are used, that they be designed in accordance with the procedure given here.

References

ASHRAE (1981), ASHRAE Handbook of Fundamentals, ASHRAE, Atlanta, Georgia.

Esch, D.C. (1978), "Road Embankment Design Alternatives Over Permafrost," Applied Techniques for Cold Environments, Vol. 1, ASCE, New York, N.Y.

Wang, F.S. (1979), "Mathematical Modeling and Computer Simulation of Insulation Systems in Below Grade Applications," ASHRAE--DOE Conference--Thermal Performance of Exterior Envelopes of Buildings, Orlando, Florida.

Johnson, P.R. and C.W. Hartman (1969), Environmental Atlas of Alaska, Institute of Water Resources, University of Alaska, College, Alaska.

Harlan, R.L. and J.F. Nixon (1968), "Ground Thermal Regime," in Geotechnical Engineering for Cold Regions, McGraw Hill, New York, N.Y.

Silberman, E. (1970), "Effect of Helix Angle on Flow in Corragated Pipes," Journal of Hydraulics Division, Vol. 96, HY11, ASCE, New York, N.Y.

Sanger, F.J. (1969), Foundations of Structures in Cold Regions, U.S. Army CRREL, Monogr. III-C4, Hanover, N.H.

Nixon, J.F. (1978), "Geothermal Aspects of Ventilated Pad Design," Proceedings Third International Permafrost Conference, Vol. 1, National Research Council of Canada, Ottawa, Canada.

List of Symbols

e = stack efficiency, 0 - 1

ϕ = lag time, days

ρ = density of air, kg/m

μ = dynamic viscosity

A = cross-sectioned area of duct

A_s = area of heated duct surface

c_p = specific heat of air

C = volumetric specific heat

D = inside duct diameter, m

f = Darcy-Weisback friction factor

F.I. = freezing index, °C-day

g = gravitational acceleration, m/s^2

h = effective height of stack, m

h_c = convective heat transfer coefficient, W/m^2 °C

i = cold air

k = soil thermal conductivity, W/m°C

K = hydraulic loss coefficients

l = length, m

L = volumetric latent heat kJ/m^3

L_e = equivalent length of duct, m

m = mass flow rate, kg/s

o = warm air

P = pressure, N/m^2

P_a = average pressure between warm and cold air

ΔP_f = frictional pressure drop

ΔP_s = stack effect pressure difference

P_v = velocity pressure

Q = heat flow per unit length, W/m

Q_t = heat flow, W

Q' = total energy, kJ

R = radius of frozen annulus, m

$\bar{R}$ = gas constant

List of Symbols (cont.)

R_e = Reynolds number
Ste = Stefan number
t = time, s
t_f = length of freezing season, days
T_{ad} = average air temperature leaving duct
T_{ed} = average air temperature entering duct
T_a = average air temperature in duct, °C
T_d = average temperature of heated duct surface, °C
T_f = temperature at the freezing point, °C
T_o = temperature 0.3 m from duct surface
T_s = ground surface temperature, °C
$\bar{T}_s$ = mean annual ground surface temperature
T_v = seasonal temperature variation
ΔT = change in temperature of air flowing through duct
V = average air velocity, m/s
w = $2\pi/365$
W = moisture content, %

APPENDIX A

Subgrade Material	Thermal Conductivity BTU/Hr-Ft-°F		Heat Capacity BTU/Ft -°F		Density Lb/Ft	Moisture % by wt.	Heat of Fusion BTU/Ft
	Frozen	Thawed	Frozen	Thawed			
Crushed Gravel	1.8	1.6	27	32	135	6%	1400
Gravel	1.6	1.1	27	37	100	20%	3000
Permafrost	1.2	0.6	28	44	75	40%	5000
Organic Silt	0.35	0.33	16	20	75	10%	1300

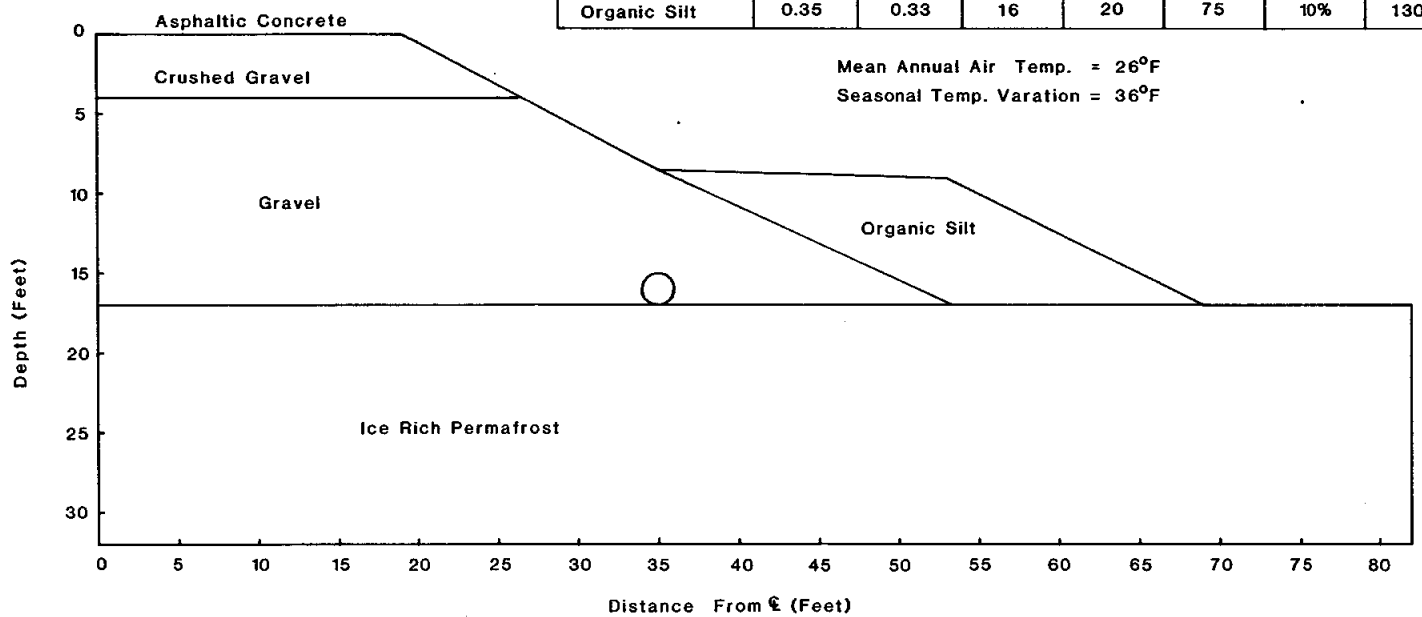

Figure A1: Air Duct System

FIGURE A2: PREDICTED TEMPERATURE PROFILE, 2′ SNOW COVER, H SURFACE AND DUCT = 4.0

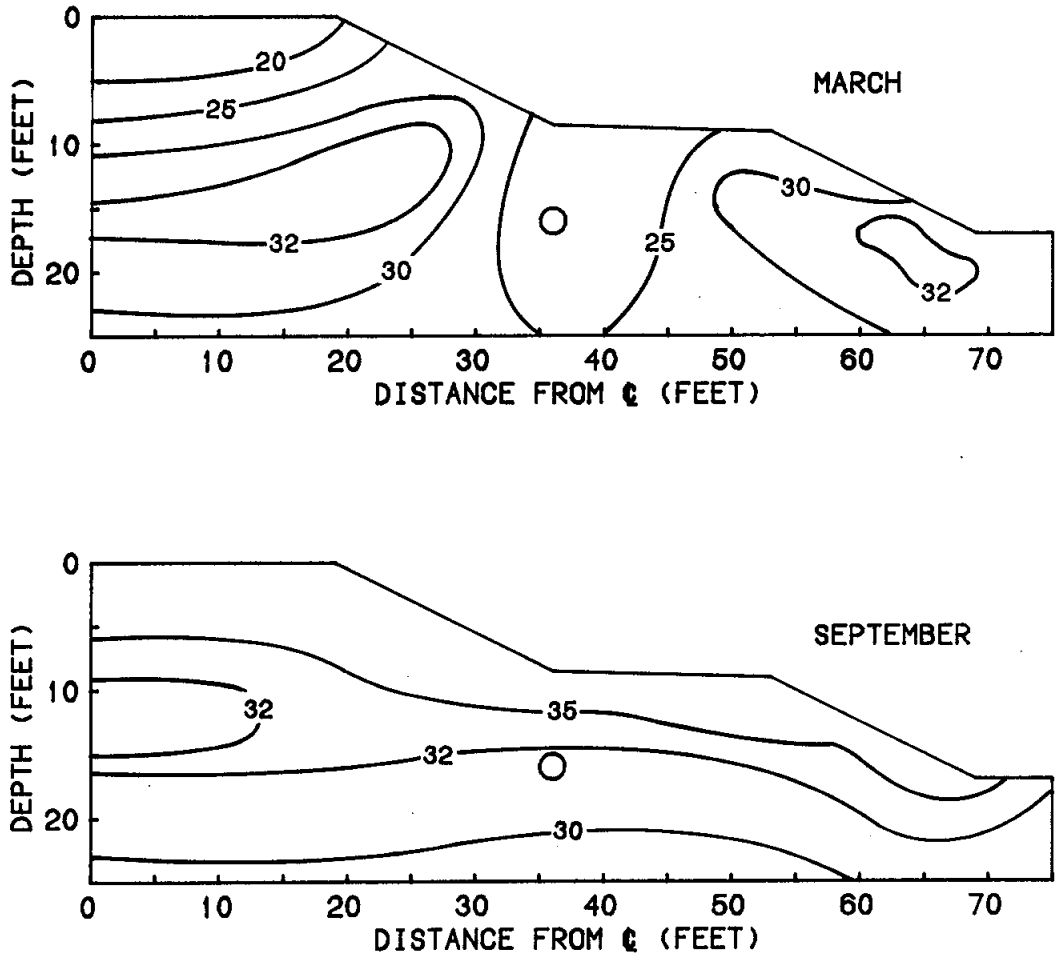

FIGURE A3: PREDICTED TEMPERATURE PROFILE, 2' SNOW COVER, H SURFACE AND DUCT = 1.7

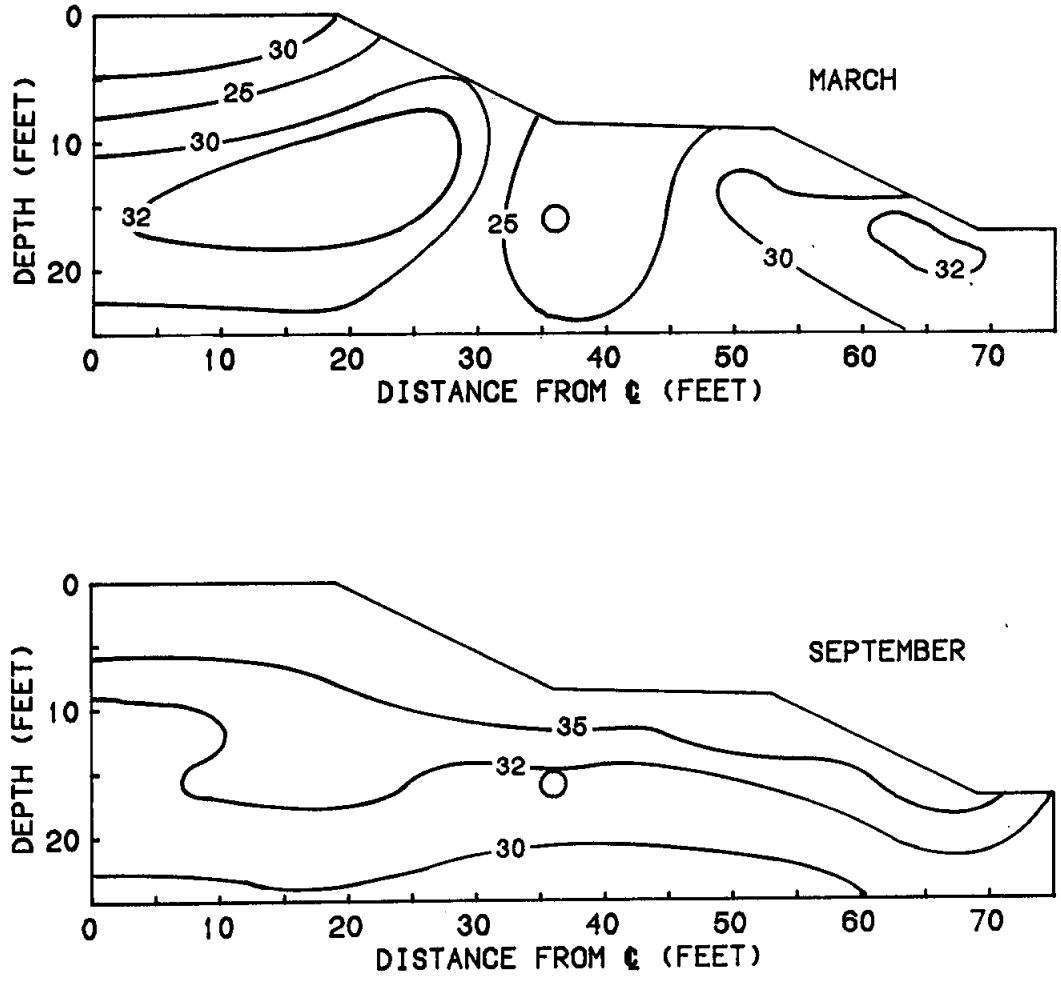

FIGURE A4: PREDICTED TEMPERATURE PROFILE, 2' SNOW COVER, H SURFACE = 4.0, NO DUCT

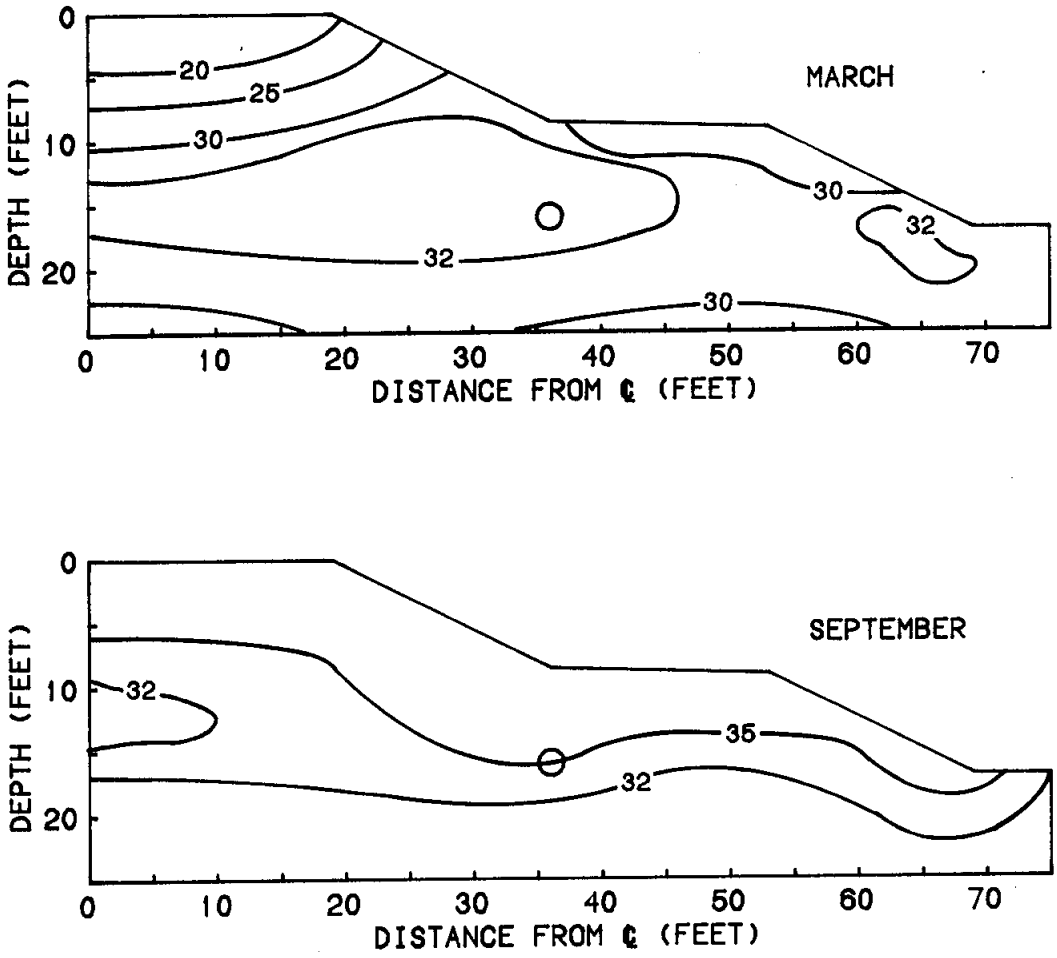

FIGURE A5: PREDICTED TEMPERATURE PROFILE, NO SNOW COVER, DUCT MOVED, H SURFACE AND DUCT = 4.0

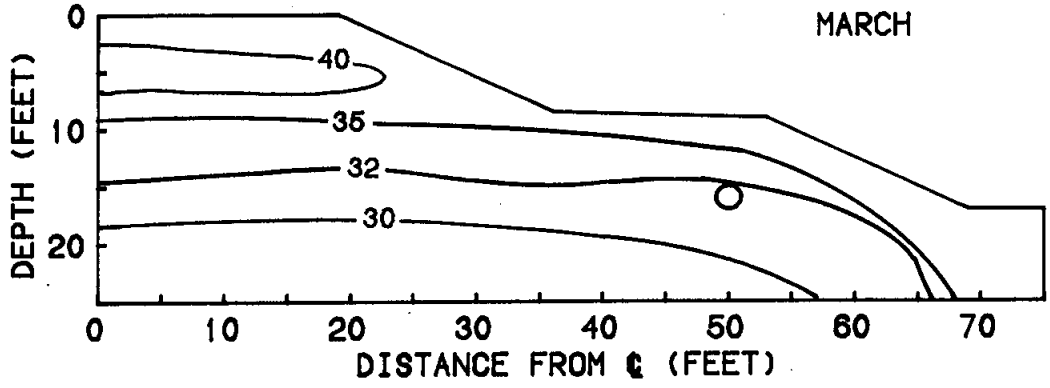

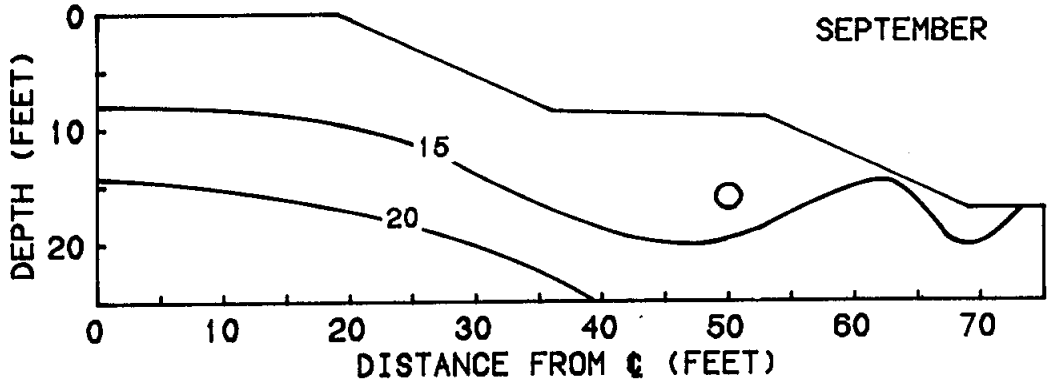

APPENDIX B

Environmental Factors

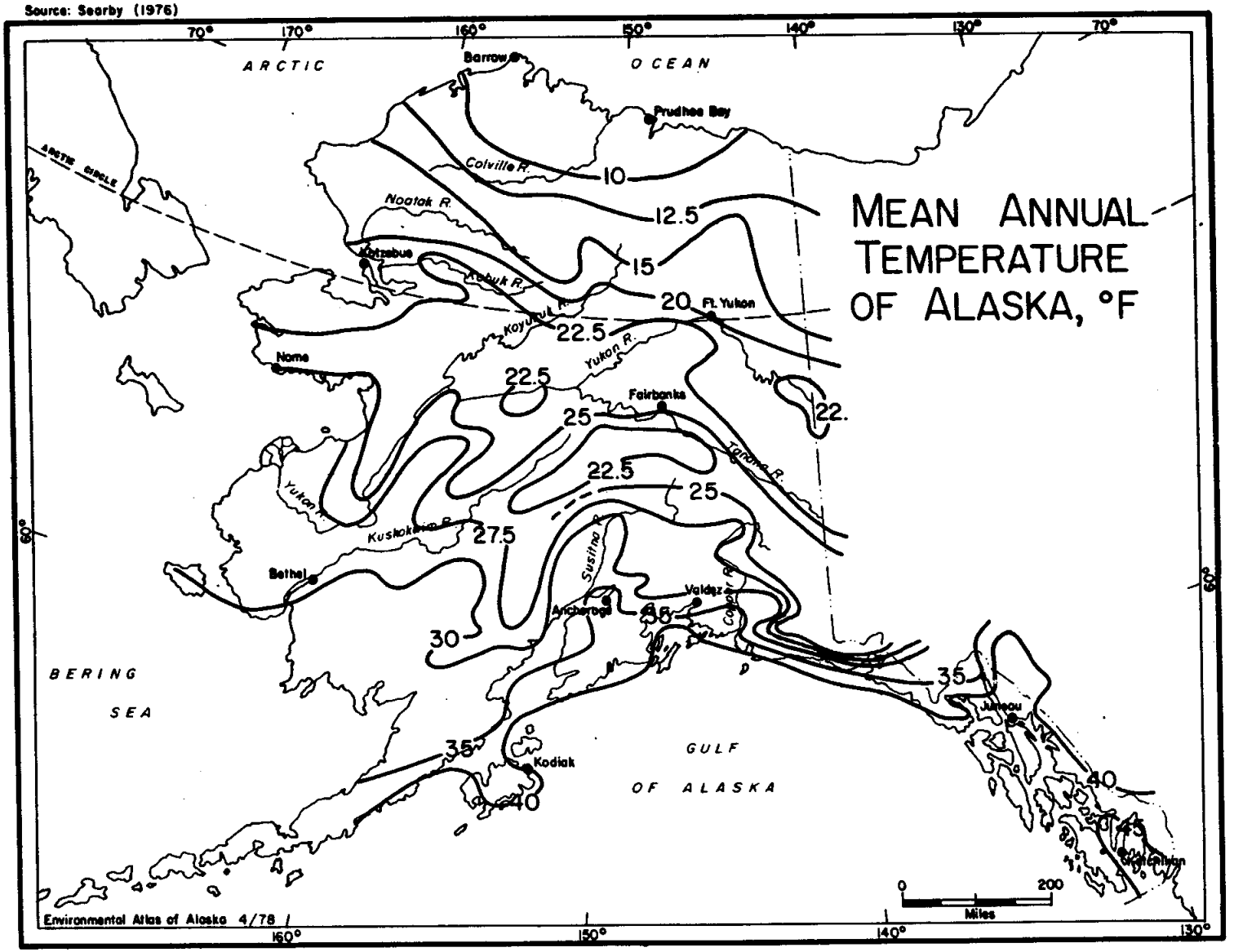

Figure B1: Mean Annual Temperature of Alaska

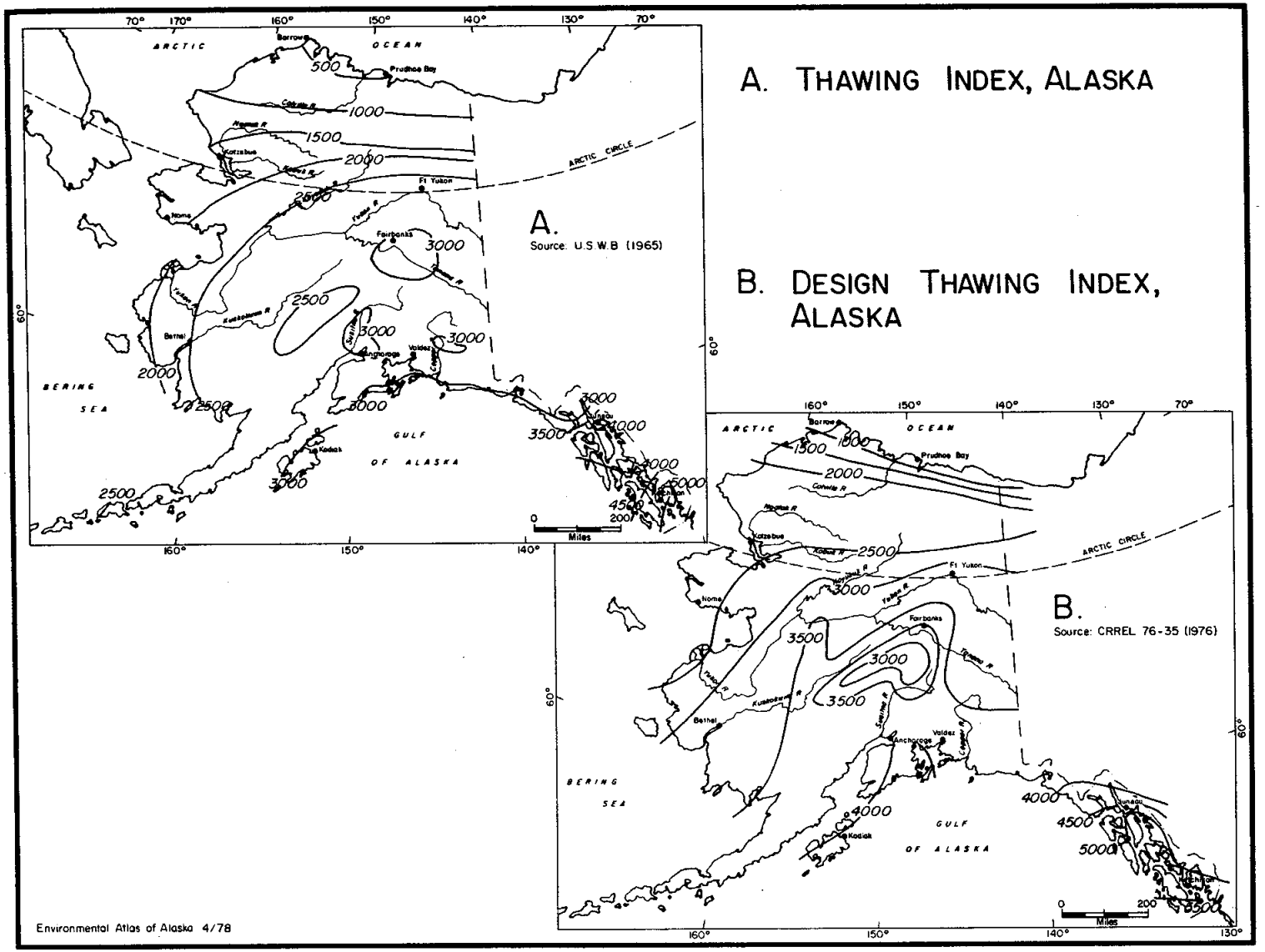

Figure B2: Thawing Index

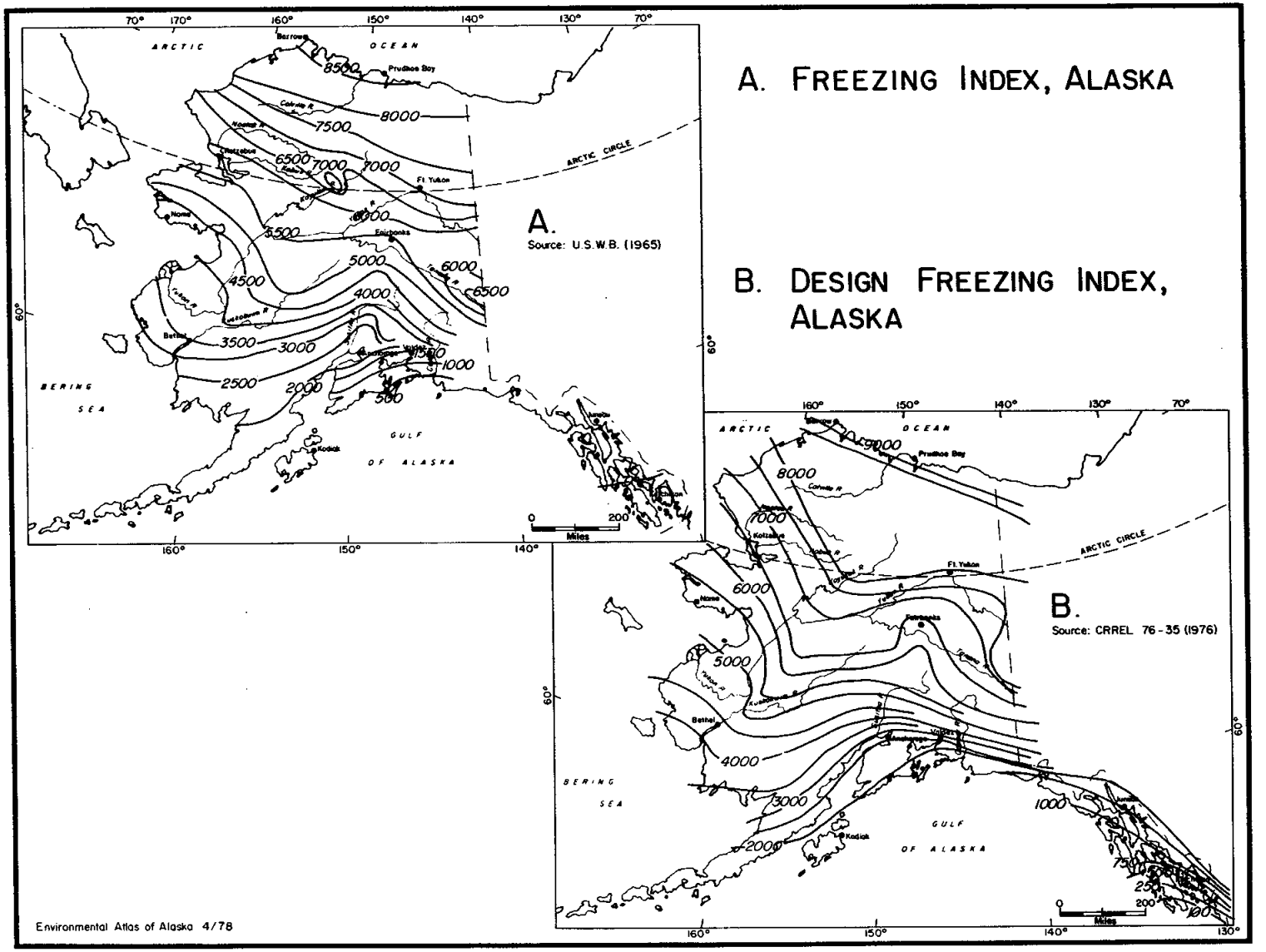

Figure B3: Freezing Index